https://doi.org/10.1137/20M136058X

SIAM J. Applied Dynamical Systems
Vol. 20, No. 4, pp. 2174–2203

Data Assimilation for the Navier–Stokes Equations Using Local Observables*

Animikh Biswas†, Zachary Bradshaw‡, and Michael S. Jolly§

Abstract. We develop, analyze, and test an approximate, *global* data assimilation/synchronization algorithm based on purely *local* observations for the two-dimensional Navier–Stokes equations on the torus. We prove that, for any error threshold, if the reference flow is analytic with sufficiently large analyticity radius, then it can be recovered within that threshold. Numerical computations are included to demonstrate the effectiveness of this approach, as well as variants with data on moving subdomains. In particular, we demonstrate numerically that machine precision synchronization is achieved for *mobile data* collected from a small fraction of the domain.

Key words. data assimilation, Navier–Stokes, local observables, mobile data

AMS subject classifications. 35Q30, 76B75, 34D06, 35Q35, 35Q93

DOI. 10.1137/20M136058X

1. Introduction.

For a given dynamical system, which is believed to accurately describe some aspect(s) of an underlying physical reality, the problem of forecasting is often hindered by inadequate knowledge of the initial state and/or model parameters describing the system. However, in many cases, such as in weather prediction, this is compensated by the fact that one has access to data from (frequently noisy) measurements of the system, collected either continuously in time or at discrete time points, albeit on a *much coarser spatial grid than the desired resolution of the forecast.* The objective of data assimilation and signal synchronization in geophysics is to use low spatial resolution observational measurements to fine tune our knowledge of the state and/or model to improve the accuracy of the forecasts [27, 51]. While atmospheric science, geoscience, and meteorology have provided the initial impetus for the subject, it has now found widespread application, including, but not limited to, environmental sciences, systems biology and medicine [54, 59], imaging science, traffic control and urban planning, economics and finance, and oil exploration [4].

An extensive literature exists on data assimilation using the Bayesian and variational framework (e.g., Kalman filters and 3DVar) [4, 16, 18, 20, 19, 45, 51, 52, 58, 70]. Despite this large body of work, as noted in [46, 75, 76], the problems of stability, accuracy, and *catastrophic*

*Received by the editors August 17, 2020; accepted for publication (in revised form) by E. Sander June 9, 2021; published electronically October 28, 2021.
https://doi.org/10.1137/20M136058X
Funding: The research of the second author was supported in part by Simons Foundation grant 635438. The research of the third author was supported in part by NSF grant DMS-1818754. This work was supported by the Lilly Endowment, Inc., through its support for the Indiana University Pervasive Technology Institute, which provided supercomputing resources used for this research.
†Mathematics & Statistics, University of Maryland Baltimore County, Baltimore, MD 21250 USA (abiswas@umbc.edu).
‡Mathematical Sciences, University of Arkansas, Fayetteville, AR 72701 USA (zb002@uark.edu).
§Department of Mathematics, Indiana University, Bloomington, IN 47405 USA (msjolly@indiana.edu).

filter divergence, particularly for infinite-dimensional chaotic dynamical systems governed by PDEs, continue to pose serious challenges to rigorous analysis of these Bayesian/Kalman filter based schemes, and are far from being resolved.

Another flexible data assimilation technique, which is analytically (and often computationally) much more tractable than variational methods (particularly 4DVar), is the so-called *nudging* (or *Newtonian relaxation*). It consists of adding an extra feedback control term to the model equation that drives the coarse mesh spatial scales of the solution toward the observed ones. This approach was used earlier in the context of feedback control of ODEs [63, 65, 74]. Subsequently, starting with [47], it has been used extensively in meteorology and oceanography as a data assimilation method; see, for instance, [15, 71, 77]. A nice survey of the use of this method in geophysics can be found in [5]. It is useful to note that for noisy data [10], nudging is a special case (with a scalar gain matrix) of the continuum level stochastic equations for 3DVar or ensemble Kalman filter [16, 52], and therefore, a thorough understanding of this method will likely help in understanding other data assimilation methods. It can also be viewed as a special case of methods used for coupling of chaotic dynamical systems in order to achieve signal synchronization; see, for instance, [69] for a nice description and survey of applications to finite-dimensional ODEs.

Though introduced earlier in geophysics and control of ODEs, to the best of our knowledge, a rigorous analytical framework for this approach for dissipative nonlinear PDEs was first developed in [6, 7]. In particular, it is shown there that due to the existence of finitely many *determining modes, nodes and volume elements* for dissipative systems, [39, 40, 25], the solution of the *data assimilation system,* i.e., the system with the added nudging term, regardless of the initial data used to initialize it, converges exponentially to the solution of the original system. Moreover, the analysis in [6, 7] provides explicit conditions on the relaxation (nudging) parameter and the spatial resolution of the observations necessary to guarantee exponential convergence to the reference solution of the model equation. This initiated a lively field of research—see [1, 10, 11, 13, 22, 34, 38, 64] and the references therein. More recently, it has been successfully implemented for efficient dynamical downscaling of a global circulation model [28], where the authors assert that "overall results clearly suggest that continuous data assimilation provides an efficient new approach for dynamical downscaling by maintaining better balance between the global model and the downscaled fields."

Rigorous results following in the vein of [6], or, for instance, [16] for variational data assimilation, are based on the earlier work on determining parameters [39, 40] and *require global knowledge*, in the form of either the low modes (which necessitates global measurements to determine) or information from a global array of uniformly distributed observables, usually nodal values or volume elements [6]. When measuring data from real world systems, certain considerations impact the placement of instruments. It is easier, for example, to measure fluid velocity or temperature at shallow depths in the ocean than at extreme depths. Similarly, a wide array of uniformly placed sensors are plainly infeasible when modeling the solar wind or the ionosphere, thus necessitating data assimilation techniques based on *local* measurements [3, 30, 31]. These examples illustrate the value of a *global* data assimilation algorithm that is based on *local* measurements. The existing abstract approaches to data assimilation require a global array of data points. In this paper, we introduce a data assimilation algorithm based on

local observables for the two-dimensional (2D) periodic Navier–Stokes equations that recovers a sufficiently regular reference solution within a specified error. The key ingredient is a spectral inequality due to Egidi and Veselić [32, 33] which bounds the L^2-norm over the full domain in terms of that over a subdomain, enabling us to use the local data obtained from the subdomain for global assimilation of the system. Moreover, we illustrate the efficacy of our algorithm by extensive computational studies. Furthermore, we demonstrate numerically that observation on a small fraction of the domain suffices for global assimilation provided the data collection domain moves with time to cover the entire domain, which may in practice indeed be the case for data collected by satellites, aircraft, or ships, which are mobile. The efficacy of *mobile data*, i.e., moving point measurements for data assimilation was also computationally observed recently by Larios and Victor [57] for a 1D model. Our numerical work shows that the same holds true for data assimilation based on local observations for the Navier–Stokes equations.

The main results are stated in section 2. After some preliminary material in section 3, we establish existence of solutions to the nudged equation in section 4, followed by the proof of synchronization in section 5. We provide in section 6 computational evidence to demonstrate the effectiveness of local sampling for the synchronization of global spatial flow features. We then test in section 7 variations of the algorithm in which the subdomain moves with time and find the convergence to the reference solution is greatly enhanced. A brief summary is given in section 8. It should be noted that while our local data assimilation results are established in the context of the Navier–Stokes equations, it is not difficult to extend these results to other dissipative fluid models such as the magnetohydrodynamic equations or the Boussinesq equations.

2. Statement of main results.

Let Ω_0 be a C^2 domain in $\mathbb{R}^2$ or the periodic box $[-L/2, L/2]^2$. The Navier–Stokes equations in functional form are

$$\frac{d}{dt}\mathbf{u} + \nu A\mathbf{u} + B(\mathbf{u},\mathbf{u}) = \mathbf{f} \text{ in } \Omega_0 \times (0,\infty); \quad \nabla\cdot\mathbf{u} = 0 \text{ in } \Omega_0 \times (0,\infty). \tag{2.1}$$

In (2.1), $B(\mathbf{u},\mathbf{v}) = \mathcal{P}(\mathbf{u}\cdot\nabla\mathbf{v})$, where $\mathcal{P}$ is the Leray projection operator, A is the Stokes operator, $\mathbf{f}$ is a given divergence-free forcing, and the velocity field $\mathbf{u}$ is unknown. We further impose zero Dirichlet boundary conditions if working on a C^2 domain and periodic boundary conditions if working on the torus. Additionally assume the flow evolves from an initial datum $\mathbf{u}_0$ in an appropriate function space. We use standard notation for the function spaces commonly used to analyze (2.1) [26, 73].

Throughout this paper we consider a domain Ω_0 and a subdomain Ω. We partition Ω in the following way: Form a lattice of points in Ω so that the distance between neighboring points is h. This leads to a finite collection of m closed squares $\{S_i\}_{i=1}^m$ so that $\Omega \subset \cup_{1\le i\le m} S_i$ and $S_i \cap \Omega \neq \emptyset$ for all $1 \le i \le m$. Let $\mathbf{x}_i$ denote the center of each square.

For our first result, let $\Omega_0 = [-L/2, L/2]^2$ and consider (2.1) with periodic boundary conditions and analytic forcing $\mathbf{f}$. Our goal is to obtain a global data assimilation result using local observables. In particular, observations are limited to an open set Ω compactly contained in Ω_0.

Two types of interpolant operators appear in the literature. Type 1 operators satisfy an approximation inequality where the upper bound involves the H^1-norm. A relevant example of a Type 1 operator is the following based on averages over volume elements:

$$(I_h f)(x) = \sum_{i=1}^{m} \chi_{S_i}(\mathbf{x})(f)_{S_i}, \tag{2.2}$$

where $(f)_{S_i}$ denotes the integral average of f over S_i, i.e., $(f)_{S_i} = \frac{1}{\text{meas}(S_i)} \int_{S_i} f$ where meas$(\cdot)$ denotes the 2D Lebesgue measure. The approximation property given in [6] for this operator is the following:

$$\|f - I_h f\|^2_{L^2(\Omega_0)} \leq c_0 h^2 \|f\|^2_{H^1(\Omega_0)}. \tag{2.3}$$

In our analysis we use a local version of this operator with an additional feature, *spectral filtering* to the first N modes. Our spectrally filtered operator is given by

$$(I_{h,N,\Omega} f)(\mathbf{x}) = P_N \sum_{i=1}^{m} \chi_{S_i \cap \Omega}(\mathbf{x})(f\chi_\Omega)_{S_i}\ , \tag{2.4}$$

where P_N is the projector onto the first N eigenvectors of A. Denoting

$$(I_{h,\Omega} f)(\mathbf{x}) = \sum_{i=1}^{m} \chi_{S_i \cap \Omega}(\mathbf{x})(f\chi_\Omega)_{S_i}, \tag{2.5}$$

we have $(I_{h,N,\Omega} f)(\mathbf{x}) = P_N (I_{h,\Omega} f)(\mathbf{x})$. Note that supp $I_{h,\Omega} f = \Omega$. An identical (modulo constants) approximation property to (2.3) will be proved in section 3 for this local operator.

Type 2 operators satisfy an approximation inequality where the upper bound involves the H^2-norm. A relevant example of a Type 2 operator is the following based on nodal values:

$$(\mathcal{I}_h f)(\mathbf{x}) = \sum_{i=1}^{m} \chi_{S_i}(\mathbf{x}) f(\mathbf{x}_i). \tag{2.6}$$

The corresponding approximation property from [6] is

$$\|f - \mathcal{I}_h f\|^2_{L^2(\Omega_0)} \leq c_0^2 (h^2 \|f\|^2_{\dot{H}^1(\Omega_0)} + h^4 \|f\|^2_{\dot{H}^2(\Omega_0)}). \tag{2.7}$$

Again, we will investigate a local version of this operator. In particular, we define

$$(\mathcal{I}_{h,N,\Omega} f)(\mathbf{x}) = P_N \sum_{i=1}^{m} \chi_{S_i \cap \Omega}(\mathbf{x})(\chi_\Omega f)(\mathbf{x}_i) = P_N \mathcal{I}_h(\chi_\Omega f). \tag{2.8}$$

Also let

$$(\mathcal{I}_{h,\Omega} f)(\mathbf{x}) = \sum_{i=1}^{m} \chi_{S_i \cap \Omega}(\mathbf{x})(\chi_\Omega f)(\mathbf{x}_i). \tag{2.9}$$

An analogous inequality to (2.7) will be proven in section 3. Spectrally filtered operators using global observables similar to these have been used for data assimilation in [23].

The interpolant operators are used to feed information about a solution $\mathbf{u}$ to (2.1) into the data assimilation equation

$$\frac{d}{dt}\mathbf{v}_N + \nu A\mathbf{v}_N + P_N B(\mathbf{v}_N, \mathbf{v}_N) = P_N\mathbf{f} - \mu(J_{h,N,\Omega}\mathbf{v}_N - J_{h,N,\Omega}\mathbf{u}), \tag{2.10}$$

where $J_{h,N,\Omega} \in \{I_{h,N,\Omega}, \mathcal{I}_{h,N,\Omega}\}$. Note that the samples used to drive $\mathbf{v}_N$ are confined to the subdomain Ω. Furthermore $\mathbf{v}_N$ lives in $\mathrm{span}(\phi_1, \dots, \phi_N)$. Our main result says that, within any given tolerance ϵ, $\mathbf{v}_N$ captures the long time properties of $\mathbf{u}$ provided N and μ are sufficiently large and h is sufficiently small, with quantities determined by Ω, ν, the Grashof number G (defined in (3.1)), and ϵ. It requires the solution $\mathbf{u}$ to be uniformly in a Gevrey class, in particular, $\mathbf{u} \in L^\infty((0,\infty); D(A^{1/2}e^{\sigma A^{1/2}}))$, with σ sufficiently large as determined by Ω, ν, G, and ϵ.

The precise definition of $D(A^{1/2}e^{\sigma A^{1/2}})$, i.e., analytic Gevrey classes, is given in section 3.2. We presently note that the (Gevrey) class $D(e^{\sigma A^{1/2}})$ coincides with real analytic functions having analyticity radius greater than or equal to σ, and although we have $D(A^{1/2}e^{\sigma A^{1/2}}) \subset D(e^{\sigma A^{1/2}})$, the analyticity radius for functions belonging to either classes is at least σ. Therefore, the classes $D(A^{s/2}e^{\sigma A^{1/2}})$ are all termed analytic Gevrey classes. The use of Gevrey norms (and corresponding Gevrey classes) was pioneered by Foias and Temam [40] for estimating the space analyticity radius for the Navier–Stokes equations and was subsequently used by many authors (see, e.g., [8] and the references therein). The Gevrey class approach enables one to avoid cumbersome recursive estimates of higher order derivatives and yields optimal estimates of the analyticity radius [66]. It has recently been used to obtain optimal decay rates for higher order Sobolev norms in [9, 8] for decaying turbulence. The conventional theory of turbulence posits the existence of certain universal length scales of paramount importance. For instance, according to Kolmogorov, there exists a *dissipation length scale*, λ_d, beyond which the viscous effects dominate the nonlinear coupling. This length scale can be characterized by the exponential decay of the energy density. Consequently, one expects the dissipation wave number, $\kappa_d = \lambda_d^{-1}$, to majorize the inertial range where energy consumption is largely governed by the nonlinear effects and dissipation can be ignored. In [12, 29] it is shown that as characterized by Gevrey norms, the (uniform) radius of spatial analyticity σ provides an estimate of the dissipation length scale, i.e., $\sigma \sim \lambda_d$.

Due to the seminal result in [40], it is well-known that, provided the forcing $\mathbf{f}$ is real analytic (for instance, if $\mathbf{f}$ is a linear combination of finitely many Fourier modes), then the global attractor (in fact a compact absorbing ball containing the global attractor) consists of real analytic functions (i.e., they belong to an appropriate Gevrey class). The analyticity radius on the attractor roughly coincides with Kolmogorov's dissipation length scale for turbulent flows. We elaborate on this condition following the statement of the theorem.

Theorem 2.1 (approximate convergence for local observations). *Let Ω be an open set in $\Omega_0 = [-L/2, L/2]^2$. Let $\mathbf{u}$ be the solution to (2.1) for some $\mathbf{u}_0 \in V$ and $\mathbf{f} \in L^\infty((0,\infty); H))$. Assume additionally that for some $\sigma > \sigma_* > 0$, where $\sigma_* = \sigma_*(\Omega)$ is an adequate constant depending on the subdomain Ω, we have*

$$M := \limsup_{t\to\infty} \|\mathbf{u}(t)\|_{D(A^{1/2}e^{\sigma A^{1/2}})} = \limsup_{t\to\infty} \|A^{1/2}e^{\sigma A^{1/2}}\mathbf{u}\|_{L^2(\Omega_0)}. \tag{2.11}$$

Let $\epsilon > 0$ be given. There exists a spectral index $N_* = N_*(G, \nu, \epsilon, M) \in \mathbb{N}$, so that, for any $N \geq N_*$, there exists a a small value $h_* = h_*(\nu, G, N)$ such that if $h \in (0, h_*)$ and $\mu \sim \frac{\nu}{h^2}$, then

$$\limsup_{t\to\infty} \|\mathbf{u}(t) - \mathbf{v}_N(t)\|_{L^2(\Omega_0)} < \epsilon,$$

where $\mathbf{v}_N$ is the global smooth solution to (2.10) taken with either $J_{h,N,\Omega} = I_{h,N,\Omega}$ or $J_{h,N,\Omega} = \mathcal{I}_{h,N,\Omega}$ and zero initial data.

Comments on Theorem 2.1.

1. The assumptions are complicated so we elaborate on how they fit together:
   (a) The needed analyticity radius σ is determined solely by the subdomain through the constant σ_*, which in turn is determined by a constant occurring in the *observation inequality* relating the local L^2-norm on the subdomain Ω to the global L^2-norm on the entire domain Ω_0. Therefore Theorem 2.1 can be viewed as saying, For analytic flows with analyticity radius sufficiently large as determined by the subdomain Ω, we can approximately recover the solution. In this sense Theorem 2.1 is a conditional result.
   (b) The best known lower estimate of the analyticity radius on the attractor is given in [55] and is of the order of $G^{-1/2}$, where G is the Grashof number. It should be noted though that in practice, the analyticity radius of the solution $\mathbf{u}(\cdot)$ can be much larger. Importantly for our theorem, once Ω_0 is fixed, if the Grashof number is taken small enough in a fashion depending on Ω_0 and the solution $\mathbf{u}$ and an analytic forcing $\mathbf{f}$ (e.g., if $\mathbf{f}$ has finitely many Fourier modes) are as in [55], then the analyticity radius σ of $\mathbf{u}$ can be made larger than the length scale σ_*.
   (c) Next, N_* is chosen large in a manner depending on ϵ, M and a priori bounded quantities associated with $\mathbf{u}$. For $N \geq N_*$, we can execute the data assimilation argument for sufficiently small h and $\mu \sim \frac{\nu}{h^2}$.
   (d) As will be apparent from the proof of Theorem 2.1 (and also Theorem 2.2), depending on the value of h (i.e., granularity of the observed data), μ can be chosen within a specified range. Choosing μ larger within this range theoretically accelerates convergence. However, setting μ too large makes the corresponding data assimilation equation stiffer, necessitating shorter time steps. Since the convergence happens at an exponential rate, in testing the capture of a known reference solution, it is evident after only a short run when an effective choice of μ has been made.
2. The existence of $\mathbf{v}_N$ is implicit in Theorem 2.1. The details are worked out in section 4.
3. If the solution $\mathbf{u}$ is replaced by a Galerkin approximation in $\text{span}(\phi_1, \ldots, \phi_N)$, then the conclusion of Theorem 2.1 holds whenever $\mathbf{f} \in L^\infty((0,\infty); H)$. Alternatively, if a condition is imposed on the forcing that results in the flow remaining spectrally local, e.g., if the forcing and data are supported on finitely many Fourier modes, then the flow can be recovered exactly as $t \to \infty$. This implies numerically simulated flows—which

are spectrally localized—can be recovered up to machine precision and round-off error using observations confined to a subdomain provided sufficiently many observations are taken. The number of observations depends exponentially on N, although as demonstrated numerically in section 6, a far smaller value of N is necessary. While this is interesting from a numeric perspective, in practical applications the observed data comes from nature and is not spectrally localized. When the flow is not spectrally local we lose exactness and also require analyticity.

4. In Azouani–Olson–Titi data assimilation, the large parameter μ is attached to a large positive global quantity and is used to hide large contributions in the energy inequality for the difference of the solution to (2.1) and the solution to the data assimilation equation. In our localized setup, μ is attached to a large positive *local* quantity while the contributions in the energy inequality remain global. To bridge the gap between global and local in this setting we use spectral inequalities developed to study control problems. These are compiled in section 3. Note that, in comparison to [6], our μ is larger in the rigorous analysis. This can be viewed as the (analytical) cost of localization, although in numerical computations, we observe that a much smaller value of μ suffices.

An exact convergence result follows as a corollary of Theorem 2.1 provided (2.11) holds and one has full knowledge of $\mathbf{u}|_\Omega$ as well as global knowledge on a set with zero space-time Lebesgue measure.[1] This means we solve

$$\frac{d}{dt}\mathbf{v}_N + \nu A\mathbf{v}_N + P_N B(\mathbf{v}_N, \mathbf{v}_N) = P_N\mathbf{f} - \mu P_N \chi_\Omega(\mathbf{v}_N - \mathbf{u}). \tag{2.12}$$

In particular, we can construct a vector field $\mathbf{v}$ that converges to $\mathbf{u}$ as $t \to \infty$ in an appropriate average sense by increasing the sample size in Theorem 2.1.

Corollary 2.1. *Under the assumptions of Theorem 2.1, i.e., (2.11), there exists a vector field $\mathbf{v} \in L^\infty((0,\infty); H) \cap L^2((0,T); V)$ for all $T > 0$ so that $\mathbf{v}$ is a limit (in an appropriate sense) of a sequence of vector fields satisfying (2.12) and for every measurable set U we have*

$$\lim_{t\to\infty} \int_U (\mathbf{u} - \mathbf{v})(\mathbf{x}, t)\, d\mathbf{x} = 0$$

at an exponential rate.

This asserts only that a vector field matching the long time behavior of $\mathbf{u}$ exists given complete local knowledge of $\mathbf{u}$. The fact that it is obtained as a limit of the solution to (2.12) means it can be approximated numerically. However, this corollary does not say what system governs $\mathbf{v}$. This is an interesting direction for future research.

We also obtain an exact data assimilation scheme for non-Gevrey forcing provided the subdomain is sufficiently large within the domain. For convenience we work with a bounded domain Ω_0 with smooth boundary and impose zero Dirichlet boundary conditions. We consider a variant of the local data assimilation equation, namely,

$$\frac{d}{dt}\mathbf{v} + \nu A\mathbf{v} + B(\mathbf{v}, \mathbf{v}) = \mathbf{f} - \mu I_{h,\Omega}(\mathbf{v} - \mathbf{u}). \tag{2.13}$$

[1] The latter can be eliminated—and hence a result given involving only data on the subdomain—but as presently written leads to a cleaner statement of the corollary.

Note that the interpolant operators are localized but there is no spectral projection. We manage this by requiring the subdomain occupy almost the full domain as this allows us to use a helpful observability inequality [78].

Theorem 2.2 (exact convergence for large subdomains). *Let $\Omega \subset \Omega_0$ be an open set with smooth boundary. Let $\mathbf{u}$ be the solution to (2.1) for some $\mathbf{u}_0 \in V$ and $\mathbf{f} \in L^\infty((0,\infty);H)$. Then there exists a small value $h_* = h_*(\nu, \Omega, \mathbf{f})$ so that, if $h \in (0, h_*)$ and $\mu \sim \frac{\nu}{h^2}$, then*

$$\|\mathbf{u}(t) - \mathbf{v}(t)\|_{L^2(\Omega_0)} \to 0, \qquad as \quad t \to \infty,$$

at an exponential rate provided $d_H(\partial\Omega, \partial\Omega_0) \sim (\sqrt{\lambda_1} G)^{-1}$, where $\mathbf{v}$ is the solution to (2.13) taken with $J_{h,N,\Omega} = I_{h,N,\Omega}$ and zero initial data, λ_1 is the first eigenvalue of the Stokes operator, and d_H denotes the Hausdorff distance between two compact sets.

As we will explain in Remark 5.3, this result allows one to avoid the collection of measurements near the (possibly turbulent) boundary layer, which may be inherently error prone. Due to Remark 5.3, $d_H(\partial\Omega, \partial\Omega_0)$ is comparable to the value h found in [6], meaning that the volume elements adjacent to the boundary of Ω_0 can be eliminated from the interpolant operators in [6]. Although this may be a small number of volume elements, they are adjacent to the boundary layer, which may be turbulent for flows with large Reynolds numbers and, consequently, subject to large measurement error. It is interesting also from a mathematical viewpoint as well, since it is an exact convergence result based on a local interpolant. As the argument is similar to Theorem 2.1, we only sketch the details of a proof—see Remarks 4.1 and 5.3

We note that the localization problem for determining nodes in the sense of [50] has been solved for analytic forcing [43, 42]. A general theme is that data assimilation implies determining quantity type results but not the other away around. For the localization problem, this appears to be the case. Indeed, the argument in [43, 42] is applied at the level of elements of the attractor, and both solutions are analytic. In data assimilation, the solution to the localized data assimilation equation does not a priori converge to the global attractor for $\mathbf{f}$. Furthermore, $\mathbf{v}_N$ is not analytic because it is driven by a term with compact support. Hence there are clear barriers to adapting the methods in [43, 42] to the data assimilation problem.

3. Preliminaries.

3.1. Strong solutions to the 2D Navier–Stokes. Recall that given $\mathbf{u}_0 \in V$ and $\mathbf{f} \in L^\infty((0,\infty);H)$, (2.1) has a unique global solution $\mathbf{u}$ so that

$$\mathbf{u} \in C([0,T];V) \cap L^2((0,T);D(A)) \text{ and } \frac{d\mathbf{u}}{dt} \in L^2((0,T);H)$$

for every $T > 0$ [26]. Furthermore we have that there exists a time $t_0 = t_0(\mathbf{u}_0)$ so that, for all $t \geq t_0$,

$$\|\mathbf{u}(t)\|^2_{L^2(\Omega_0)} \leq 2\nu^2 G^2 \text{ and } \int_t^{t+T} \|A^{1/2}\mathbf{u}(s)\|^2_{L^2(\Omega_0)}\, ds \leq 2(1 + T\nu\lambda_1)\nu G^2,$$

where $T > 0$ is fixed and G denotes the Grashof number which is defined to be

$$G = \frac{1}{\nu^2 \lambda_1} \limsup_{t\to\infty} \|\mathbf{f}(t)\|_{L^2(\Omega_0)}. \tag{3.1}$$

The above are true for both Dirichlet boundary conditions on a bounded domain with C^2 boundary or for periodic boundary conditions. For the periodic case we have the following improvement: There exists a time $t_0 = t_0(\mathbf{u}_0)$ so that, for all $t \geq t_0$,

$$\|A^{1/2}\mathbf{u}(t)\|^2_{L^2(\Omega_0)} \leq 2\nu^2\lambda_1 G^2 \text{ and } \int_t^{t+T} \|A\mathbf{u}(s)\|^2_{L^2(\Omega_0)}\, ds \leq 2(1+T\nu\lambda_1)\nu\lambda_1 G^2, \tag{3.2}$$

where $T > 0$ is fixed.

3.2. L^2 Gevrey classes. Recall that if $\mathbf{u} \in L^2(\Omega_0)$ is periodic and has zero mean and $\Omega_0 = [-L/2, L/2]^2$, then

$$\mathbf{u}(\mathbf{x}) = \sum_{\mathbf{k}\in\mathbb{Z}^2\setminus\{0\}} \hat{\mathbf{u}}_{\mathbf{k}} e^{\frac{2\pi i}{L}\mathbf{k}\cdot\mathbf{x}},$$

where

$$\hat{\mathbf{u}}_{\mathbf{k}} = \int_{\Omega_0} \mathbf{u}(\mathbf{y}) e^{-\frac{2\pi i}{L}\mathbf{k}\cdot\mathbf{y}}\, d\mathbf{y}.$$

Working on the periodic box $[-L/2, L/2]^2$, we define the Gevrey spaces $D(A^r e^{\sigma A^s})$ to be those elements of H satisfying

$$\|\mathbf{u}\|^2_{D(A^r e^{\sigma A^s})} := L^2 \sum_{k\in\mathbb{Z}^2} \left|\frac{k}{L}\right|^{4r} e^{2\sigma|2\pi\frac{k}{L}|^{2s}} |\hat{\mathbf{u}}_{\mathbf{k}}|^2 < \infty.$$

Analyticity corresponds to $r = 0$ and $s = 1/2$. We only use $r = 0$ and $s = 1/2$ or $r = s = 1/2$. Note that for Gevrey class forcing, a solution $\mathbf{u}$ to (2.1) becomes and remains Gevrey regular for positive times. Indeed, for large enough times we have the following uniform bound [37, p. 74]:

$$|\hat{\mathbf{u}}_{\mathbf{k}}|^2 \leq C\lambda_1\nu^2|\mathbf{k}|^{-2} e^{-4\pi\delta_0|\mathbf{k}|/L}[1+G^2],$$

where δ_0 is inversely related to G. For our applications, this is insufficient unless G is taken to be small, so we impose an explicit assumption that the analyticity radius is large when G is not small. In particular, we assume

$$\limsup_{t\to\infty} \|\mathbf{u}(t)\|_{D(A^{1/2}e^{\sigma A^{1/2}})} =: M < \infty,$$

where σ is as in Theorem 2.1 and

$$\|\mathbf{u}(t)\|_{D(A^{1/2}e^{\sigma A^{1/2}})} = |A^{1/2}e^{\sigma A^{1/2}}\mathbf{u}|.$$

The preceding condition implies

$$\limsup_{t\to\infty} |\hat{\mathbf{u}}_{\mathbf{k}}|^2(t) \leq M^2|\mathbf{k}|^{-2} e^{-4\pi\sigma|\mathbf{k}|/L}.$$

Gevrey class and analytic solutions to (2.1) and other fluid models have been studied extensively. A partial list is [14, 17, 21, 41, 44, 55].

3.3. The Stokes operator. We denote by ϕ_i the eigenvectors and λ_i the eigenvalues of the Stokes operator. P_N denotes the projection operator from L^2 onto $\text{span}(\phi_1, \dots, \phi_N)$.

Recall from [26] that for periodic domains and restricting to functions with zero mean, the Stokes operator A agrees with $-\Delta$. Furthermore, abusing notation slightly, the eigenfunctions $\phi_{\mathbf{k}}$ of A can be written explicitly in terms of $\{e^{2\pi i \frac{\mathbf{k}}{L}\cdot\mathbf{x}}\}_{\mathbf{k}\in\mathbb{Z}^2}$ as

$$\phi_{\mathbf{k}} = a_{\mathbf{k}} L^{-1} e^{2\pi i \frac{\mathbf{k}}{L}\cdot\mathbf{x}} + \bar{a}_{\mathbf{k}} L^{-1} e^{-2\pi i \frac{\mathbf{k}}{L}\cdot\mathbf{x}},$$

where $a_{\mathbf{k}} \in \mathbb{C}^2$ satisfy $a_{\mathbf{k}} \cdot \mathbf{k} = 0$. For each $\mathbf{k} \in \mathbb{Z}^2 \setminus \{0\}$ there are actually two eigenfunctions of the above form but we suppress this. Note that $\{\phi_{\mathbf{k}}\}$ is orthonormal and all elements have mean zero. The eigenvalues of A are the values $4\pi^2 L^{-2}|\mathbf{k}|^2$ for $\mathbf{k} \in \mathbb{Z}^2 \setminus 0$. The eigenfunctions can be ordered as $\{\phi_j\}_{j\in\mathbb{N}}$ so that the corresponding eigenvalues λ_j are nondecreasing. By symmetry, the multiplicity of the eigenvalue λ_j is

$$\#\{\mathbf{k} \in \mathbb{Z}^2 : |\mathbf{k}|^2 = \lambda_j \lambda_1^{-1}\}.$$

If we are given an eigenvalue λ_j, then this corresponds to points $\mathbf{k} \in \mathbb{Z}^2 \setminus \{0\}$ in the square $[-K, K]^2$ where $K^2 \sim j$. Furthermore, we have asymptotically that

$$\lambda_j \lesssim j,$$

implying

$$K^2 \lesssim j.$$

Plainly then, if $\mathbf{u} \in \text{span}(\phi_1, \dots, \phi_N)$, there exists $K \sim \sqrt{N}$ so that $\hat{\mathbf{u}}$ is supported in $[-K, K]^2$.

For other properties of the Stokes operator, as well as its eigenvectors and eigenvalues, see [37, II.6] as well as [26, 73].

3.4. Approximation property of local interpolant operators. We prove analogues of (2.3) and (2.7) for local interpolant operators. The local volume interpolant operator (2.5) satisfies the approximation property

$$\|I_{h,\Omega} f - f\|^2_{L^2(\Omega)} \le c_0 h^2 \|f\|^2_{H^1(\Omega_0)}. \tag{3.3}$$

Structurally this is identical to (2.3) but the operator is local so we check details. By the Poincaré inequality,

$$\|I_{h,\Omega} f - f\|^2_{L^2(\Omega)} \le \sum_{i=1}^{m} \text{meas}(S_i \cap \Omega) C_{S_i\cap\Omega} \|\nabla(f\chi_\Omega)\|^2_{L^2(S_i\cap\Omega)},$$

where $C_{S_i\cap\Omega}$ is the Poincaré constant for $S_i \cap \Omega$. These constants are uniformly bounded because the sets $C_{S_i\cap\Omega}$ all have bounded diameters. We thus obtain

$$\|I_{h,\Omega} f - f\|^2_{L^2(\Omega)} \le c_0 h^2 \sum_{i=1}^{m} \|\nabla f\|^2_{L^2(S_i\cap\Omega)} = c_0 h^2 \|f\|^2_{H^1(\Omega)} \le c_0 h^2 \|f\|^2_{H^1(\Omega_0)},$$

which is (3.3).

The local nodal interpolant operator (2.9) satisfies the approximation property

$$\|\mathcal{I}_{h,\Omega} f - f\|^2_{L^2(\Omega)} \leq c_0^2 (h^2 \|f\|^2_{\dot{H}^1(\Omega_0)} + h^4 \|f\|^2_{H^2(\Omega_0)}). \tag{3.4}$$

Again, this follows essentially the original argument in [6] which is adapted from [50]. Recall from [50, 6] that if Q is a square of side length h and $\mathbf{x}, \mathbf{y} \in Q$, then for $f \in H^2(Q)$,

$$|f(\mathbf{x}) - f(\mathbf{y})| \leq 2\left(4\|\nabla f\|^2_{L^2(Q)} + h^2 \|Af\|^2_{L^2(Q)}\right)^{1/2}. \tag{3.5}$$

Then, following [6, p. 299],

$$\begin{aligned} \|f - \mathcal{I}_{h,\Omega} f\|^2_{L^2(\Omega)} &\leq \sum_{i=1}^m \int |f(\mathbf{x}) - f(\mathbf{x}_i)|^2 \chi_{S_i}(\mathbf{x}) d\mathbf{x} \\ &\leq \sum_{i=1}^m 4h^2 \big(4\|f\|^2_{\dot{H}^1(S_i)} + h^2 \|f\|^2_{\dot{H}^2(S_i)}\big) \\ &\leq c_0^2 (h^2 \|f\|^2_{\dot{H}^1(\Omega_0)} + h^4 \|f\|^2_{\dot{H}^2(\Omega_0)}). \end{aligned} \tag{3.6}$$

3.5. Spectral inequalities. For our approximate data assimilation result, we use a spectral inequality of Egidi and Veselić for the torus [32, 33]. This extends earlier work on $\mathbb{R}^d$ [53]. The spectral inequality applies to "thick" sets. A set S is thick in $\mathbb{R}^2$ if there exists $\gamma \in (0, 1]$ and $a = (a_1, a_2)$ where $a_i > 0$ so that for every $\mathbf{x} \in \mathbb{R}^2$,

$$|(S + \mathbf{x}) \cap ([0, a_1] \times [0, a_2])| \geq \gamma a_1 a_2 \, .$$

It is easy to see that any open set in $[-L/2, L/2]^2$ which is periodically extended to $\mathbb{R}^2$ is thick. The spectral theorem on the torus is the following.

Theorem 3.1 (see [32]). *Let $f \in L^2(\Omega_0)$ where Ω_0 denotes the torus $[0, L_1] \times [0, L_2]$. Assume* supp $\hat{f} \subset J$ *where J is a rectangle in $\mathbb{R}^2$ with sides parallel to coordinate axes and of length b_1 and b_2. Let $b = (b_1, b_2)$. Let $S \subset \mathbb{R}^2$ be a (γ, a)-thick set with $a = (a_1, a_2)$ so that $0 < a_j < 2\pi L_j$ for $j = 1, 2$. Then*

$$\|f\|_{L^2(\Omega_0)} \leq C\gamma^{-ca\cdot b - \frac{13}{2}} \|f\|_{L^2(S \cap \Omega_0)}.$$

For simplicity we take $L_1 = L_2 = L$ and S to be the periodic extension of a ball with radius $r < L/2$ to all of $\mathbb{R}^2$. It is not difficult to see that this set is thick with

$$a_i = L - r \qquad \text{and} \qquad \gamma = \frac{\pi r^2}{4(L - r)^2} \, .$$

We can also take $b_1 = b_2 = 2K$ where $K \in \mathbb{N}$ is fixed and J centered at the origin. Then, for any open set Ω contained in Ω_0, we have as a consequence of Theorem 3.1 applied to a ball of radius r contained in Ω_0 that

$$\sum_{\mathbf{k} \in [-K,K]^2 \cap \mathbb{Z}^2} |\tilde{f}_{\mathbf{k}}|^2 \leq C\gamma^{-2c(L-r)K - 13} \int_\Omega \left| \sum_{\mathbf{k} \in [-K,K]^2 \cap \mathbb{Z}^2} \tilde{f}_{\mathbf{k}} e^{2\pi i \frac{k}{L} \cdot \mathbf{x}} \right|^2 d\mathbf{x}, \tag{3.7}$$

where $\tilde{f}_{\mathbf{k}}$ is the Fourier coefficient for $\mathbf{k} \in \mathbb{Z}^2$. We prefer to rewrite this inequality in the form

$$\|f\|^2_{L^2(\Omega_0)} \leq C_\Omega e^{C_\Omega K} \|f\|^2_{L^2(\Omega)}, \tag{3.8}$$

where C_Ω represents positive constants which are independent of K and range $\hat{f} \subset [-K, K]^2$. Based on the discussion in section 3.3, we can also formulate this result in terms of the Stokes operator: If $f \in \text{span}(\phi_1, \ldots, \phi_N)$, then

$$\|f\|^2_{L^2(\Omega_0)} \leq C_\Omega e^{C_\Omega \sqrt{N}} \|f\|^2_{L^2(\Omega)}. \tag{3.9}$$

For bounded domains, there is a spectral inequality for the Stokes operator due to Chaves-Silva and Lebeau [24].

Theorem 3.2 (see [24]). *Let $\Omega \subset \Omega_0$ be a nonempty open set. There exist constants $M > 0$ and $K > 0$ so that for every sequence of complex numbers z_j and every real $\Lambda > 0$ we have*

$$\sum_{\lambda_j \leq \Lambda} |z_j|^2 = \int_{\Omega_0} \left| \sum_{\lambda_j \leq \Lambda} z_j \phi_j \right|^2 dx \leq M e^{K\sqrt{\Lambda}} \int_{\Omega} \left| \sum_{\lambda_j \leq \Lambda} z_j \phi_j(\mathbf{x}) \right|^2 d\mathbf{x}, \tag{3.10}$$

where ϕ_j are the eigenvectors and λ_j are the eigenvalues of the Stokes operator.

Spectral inequalities of this form were established earlier for elliptic operators on a bounded domain in [62, 60] using Carleman inequalities and a pointwise interpolation estimate from [61]. Although in Theorem 2.1 we consider only the case of the periodic boundary conditions, similar techniques can be employed for the bounded domain as well—see Remark 5.1.

3.6. An observation inequality. Theorem 2.2 is an exact convergence result when the observation domain is almost the entire domain. Our main technical tool for this is the following observation inequality due to Yu and Li [78].

Lemma 3.1 (see [78]). *Let Ω and Ω_0 be bounded domains with smooth boundary so that $\Omega \subset \Omega_0$. For any $\epsilon > 0$, there exists $K(\epsilon) > 0$ so that for $k > K$, the following inequality holds:*

$$\int_{\Omega_0} |\nabla u|^2 + k\chi_\Omega |u|^2 \, d\mathbf{x} \geq (\lambda_1(\Omega) - \epsilon) \int_{\Omega_0} |u|^2 \, d\mathbf{x} \tag{3.11}$$

for $u \in H^1_0(\Omega_0)$ and λ_1 the first eigenvalue of the Laplace operator on the domain $\Omega_0 \setminus \overline{\Omega}$ with zero-Dirichlet boundary conditions. As $|\Omega| \to |\Omega_0|$, $\lambda_1(\Omega)$ increases without bound.

As a final comment let us note that an observation inequality for (2.1) is given in [49] for the difference of two solutions. There are, however, major obstacles to applying the observation inequality of [49] to the difference of the reference solution and the data assimilation solution. In particular, the observation inequality in [49] involves many parameters which, in our application, must remain bounded as $t \to \infty$. In [49], these parameters are only required to satisfy the referenced bounds on a short time interval. This is enough for the purposes of [49], as their goal is to prove uniqueness, while they are insufficient here as our goal is to obtain asymptotic convergence.

4. Solving the data assimilation equations. In this section we construct solutions to the data assimilation equations introduced in section 1. Recall the data assimilation equation is

$$\frac{d}{dt}\mathbf{v}_N + \nu A\mathbf{v}_N + P_N B(\mathbf{v}_N, \mathbf{v}_N) = P_N\mathbf{f} - \mu J_{h,N,\Omega}(\mathbf{v}_N - \mathbf{u}), \tag{4.1}$$

where $J_{h,N,\Omega}$ is either $I_{h,N,\Omega}$ or $\mathcal{I}_{h,N,\Omega}$. We focus on periodic boundary conditions and assume $\mathbf{f} \in L^\infty((0,\infty); H)$. Notice that the data assimilation equation has the form

$$\frac{d}{dt}\mathbf{v}_N + \nu A\mathbf{v}_N = F_N(\mathbf{u}, \mathbf{v}_N, \mathbf{f}),$$

where $F_N \in \operatorname{span}(\phi_1, \dots, \phi_N)$. Provided the data $\mathbf{v}_{N0}$ is also in $\operatorname{span}(\phi_1, \dots, \phi_N)$, we may seek a solution $\mathbf{v}_N(t) \in \operatorname{span}(\phi_1, \dots, \phi_N)$ for all t. Formally taking $\mathbf{v}_N(t) \in \operatorname{span}(\phi_1, \dots, \phi_N)$ for all t results in a finite system of ODEs which possesses a local-in-time unique strong solution. We take $\mathbf{v}_N$ to be this solution and let $T(\mathbf{v}_{N0})$ be the maximal existence time for $\mathbf{v}_N$ for data $\mathbf{v}_{N0}$. Since the solution is strong, we have $\mathbf{v}_N \in C([0, T(\mathbf{v}_{N0})); H)$. Note that if $T(\mathbf{v}_{N0})$ is maximal and finite, then the L^2-norm of $\mathbf{v}_N$ must blow up at $T(\mathbf{v}_{N0})$. Hence, a uniform in time bound for the L^2-norm implies $T(\mathbf{v}_{N0}) = \infty$. The next lemma provides such a bound and implies $\mathbf{v}_N$ is a global solution provided h is sufficiently small.

Lemma 4.1. *Let $\mathbf{u}_0 \in V$ be given and let $\mathbf{u}$ be the solution to (2.1) for data $\mathbf{u}_0 \in V$ and $\mathbf{f} \in L^\infty((0,\infty); H)$. Fix $N \in \mathbb{N}$, $h > 0$, and $\mu > 0$ and $J_{h,N,\Omega} \in \{I_{h,N,\Omega}, \mathcal{I}_{h,N,\Omega}\}$. Assume $\mathbf{v}_{N0} \in \operatorname{span}(\phi_1, \dots, \phi_N)$ and let $\mathbf{v}_N$ be the unique strong solution to (2.10) on $[0, T(\mathbf{v}_{N0}))$ for some $h > 0$. Then, provided h is sufficiently small, $\mathbf{v}_N$ satisfies*

$$\mathbf{v}_N \in L^\infty((0, T(\mathbf{v}_{N0})); H) \cap L^2((0, T'); V) \tag{4.2}$$

for every $0 < T' < T(\mathbf{v}_{N0})$. The first inclusion implies $T(\mathbf{v}_{N0}) = \infty$.

For type 1 interpolants, the requirement on h in [6] is $2\mu c_0 h^2 \le \nu$. This is better than ours by a factor of 4.

Because $\mathbf{v}_N$ is confined to $\operatorname{span}(\phi_1, \dots, \phi_N)$, we may deduce bounds on higher order derivatives freely using properties of the eigenvectors of the Stokes operator. Hence we do not need to prove such estimates as required in [6].

We do not require any Gevrey regularity of $\mathbf{f}$ at this point.

Proof. We first focus on $J_{h,N,\Omega} = I_{h,N,\Omega}$. Take the inner product of (2.10) with $\mathbf{v}_N$ and integrate in space to obtain

$$\frac{1}{2}\frac{d}{dt}\|\mathbf{v}_N\|^2_{L^2(\Omega_0)} + \nu\|A^{1/2}\mathbf{v}_N\|^2_{L^2(\Omega_0)} = (\mathbf{f} + \mu I_{h,N,\Omega}\mathbf{u}, \mathbf{v}_N) - \mu(I_{h,N,\Omega}\mathbf{v}_N, \mathbf{v}_N),$$

where $(\cdot,\cdot) = (\cdot,\cdot)_{L^2(\Omega_0)}$. We estimate each term on the right-hand side. For the source terms we have

$$|(\mathbf{f}, \mathbf{v}_N)| \le \frac{4}{\nu\lambda_1}\|\mathbf{f}\|^2_{L^2(\Omega_0)} + \frac{\nu}{4}\|A^{1/2}\mathbf{v}_N\|^2_{L^2(\Omega_0)}$$

and

$$|(\mu I_{h,N,\Omega}\mathbf{u}, \mathbf{v}_N)| \le \frac{4\mu^2}{\nu\lambda_1}\|I_{h,\Omega}\mathbf{u}\|^2_{L^2(\Omega_0)} + \frac{\nu}{4}\|A^{1/2}\mathbf{v}_N\|^2_{L^2(\Omega_0)},$$

where we used the fact that $\mathbf{v}_N$ is projected onto the first N modes to eliminate P_N in the inner product. A direct computation confirms that

$$\|I_{h,\Omega}\mathbf{u}\|^2_{L^2(\Omega_0)} \leq \|\mathbf{u}\|^2_{L^2(\Omega_0)},$$

where we used (2.3). Hence

$$|(\mu I_{h,N,\Omega}\mathbf{u}, \mathbf{v}_N)| \leq \frac{4\mu^2}{\nu\lambda_1}\|\mathbf{u}\|^2_{L^2(\Omega_0)} + \frac{\nu}{4}\|A^{1/2}\mathbf{v}_N\|^2_{L^2(\Omega_0)}.$$

For the remaining term we have

$$-\mu(I_{h,N,\Omega}\mathbf{v}_N, \mathbf{v}_N) = -\mu(I_{h,\Omega}\mathbf{v}_N, \mathbf{v}_N) = -\mu(I_{h,\Omega}\mathbf{v}_N - \chi_\Omega\mathbf{v}_N, \mathbf{v}_N) - \mu\int_\Omega |\mathbf{v}_N|^2\, d\mathbf{x}. \tag{4.3}$$

The last term above has a good sign while, using (3.3), the second to last is bounded as

$$\begin{aligned}\mu|(I_{h,\Omega}\mathbf{v}_N - \chi_\Omega\mathbf{v}_N, \mathbf{v}_N)| &\leq \mu\|I_{h,\Omega}\mathbf{v}_N - \chi_\Omega\mathbf{v}_N\|_{L^2(\Omega_0)}\|A^{1/2}\mathbf{v}_N\|_{L^2(\Omega)} \\ &\leq 2\mu c_0 h^2\|A^{1/2}\mathbf{v}_N\|^2_{L^2(\Omega_0)} + \frac{\mu}{2}\|\mathbf{v}_N\|^2_{L^2(\Omega)}.\end{aligned} \tag{4.4}$$

We now require

$$2\mu c_0 h^2 \leq \frac{\nu}{4}. \tag{4.5}$$

Granting this and absorbing terms where possible we obtain

$$\frac{1}{2}\frac{d}{dt}\|\mathbf{v}_N\|^2_{L^2(\Omega_0)} + \frac{\nu}{4}\|A^{1/2}\mathbf{v}_N\|^2_{L^2(\Omega_0)} \leq \frac{4}{\nu\lambda_1}\|\mathbf{f}\|^2_{L^2(\Omega_0)} + \frac{4\mu^2}{\nu\lambda_1}\|\mathbf{u}\|^2_{L^2(\Omega_0)} - \frac{\mu}{2}\|\mathbf{v}_N\|^2_{L^2(\Omega)}. \tag{4.6}$$

Using the Poincaré inequality and dropping the term with a good sign we have

$$\frac{1}{2}\frac{d}{dt}\|\mathbf{v}_N\|^2_{L^2(\Omega_0)} + \frac{\nu\lambda_1}{4}\|\mathbf{v}_N\|^2_{L^2(\Omega_0)} \leq \frac{4}{\nu\lambda_1}\|\mathbf{f}\|^2_{L^2(\Omega_0)} + \frac{4\mu^2}{\nu\lambda_1}\|\mathbf{u}\|^2_{L^2(\Omega_0)}. \tag{4.7}$$

Since the right-hand side is uniformly bounded in t, this leads to a uniform in time bound on $|\mathbf{v}_N|$ in the usual way [6]. Note that this bound is independent of N.

The proof is the same if we replace $I_{h,N,\Omega}$ with $\mathcal{I}_{h,N,\Omega}$ with one modification: Instead of (4.4) we have

$$\begin{aligned}\mu|(\chi_\Omega\mathbf{v}_N - \mathcal{I}_{h,\Omega}\mathbf{v}_N, \mathbf{v}_N)| &\leq \mu\|\chi_\Omega\mathbf{v}_N - \mathcal{I}_{h,\Omega}\mathbf{v}_N\|_{L^2(\Omega_0)}\|\mathbf{v}_N\|_{L^2(\Omega_0)} \\ &\leq 2\mu c_0^2 h^2\|\mathbf{v}_N\|^2_{\dot{H}^1(\Omega_0)} + 2\mu c_0^2 h^4\|\mathbf{v}_N\|^2_{\dot{H}^2(\Omega_0)} + \frac{\mu}{2}\|\mathbf{v}_N\|^2_{L^2(\Omega)} \\ &\leq 2\mu c_0^2(h^2 + h^4\lambda_N)\|A^{1/2}\mathbf{v}_N\|^2_{L^2(\Omega_0)} + \frac{\mu}{2}\|\mathbf{v}_N\|^2_{L^2(\Omega)}.\end{aligned} \tag{4.8}$$

After fixing N and μ we therefore take h small so that $2\mu c_0^2(h^2 + h^4\lambda_N) < \frac{\nu}{4}$ and proceed as in the case of $I_{h,N,\Omega}$. ∎

Remark 4.1. We discuss the existence problem for (2.13). Because the localization in (2.13) does not involve a spectral projection, it is very similar to the usual existence result [6], using the usual Galerkin approximation procedure. Therefore we include only the needed a priori bound and direct the reader to [6] as well as [26, 73] for more details. For the a priori bound, starting with (2.13) we have

$$\frac{1}{2}\frac{d}{dt}\|\mathbf{v}_N\|^2_{L^2(\Omega_0)} + \nu\|A^{1/2}\mathbf{v}_N\|^2_{L^2(\Omega_0)} = (\mathbf{f},\mathbf{v}_N) - \mu(I_{h,\Omega}\mathbf{v}_N,\mathbf{v}_N) + \mu(I_{h,\Omega}\mathbf{u},\mathbf{v}_N).$$

As in the proof of Proposition *4.1*, the source terms lead to time-independent quantities on the right-hand side while

$$-\mu(I_{h,\Omega}\mathbf{v}_N,\mathbf{v}_N) = -\mu(I_{h,\Omega}\mathbf{v}_N - \chi_\Omega\mathbf{v}_N,\mathbf{v}_N) - \mu\|\mathbf{v}_N\|^2_{L^2(\Omega)}.$$

This is identical to (4.3) and we can conclude following the identical argument. In particular, for μ fixed and h chosen to satisfy $8\mu c_0 h^2 \le \nu$, we obtain a uniform bound on $\mathbf{v}_N$ in terms of μ, $\mathbf{u}$, and $\mathbf{f}$. To rigorously construct a solution, we would now apply this a priori bound to a Galerkin scheme and pass to the limit using the standard compactness argument.

This existence result does not require Ω to occupy most of Ω_0. This constraint will be needed for data assimilation.

5. Local data assimilation.

Proof of Theorem 2.1. Let $\epsilon > 0$ be given. Let $\bar{\epsilon} = \frac{\epsilon\nu\lambda_1}{8}$. Let $\mathbf{u}$ and $\mathbf{v}_N$ be as in the statement of Theorem 2.1. Note that for any $N \in \mathbb{N}$, $P_N\mathbf{u}$ solves

$$\frac{d}{dt}P_N\mathbf{u} + \nu AP_N\mathbf{u} + P_NB(P_N\mathbf{u},\mathbf{u}) = P_N\mathbf{f} - P_NB(Q_N\mathbf{u},\mathbf{u}), \tag{5.1}$$

where $Q_N = I - P_N$. We will eventually specify a value for N.

Let $\mathbf{w} = \mathbf{v}_N - P_N\mathbf{u}$. Then $\mathbf{w}$ is divergence free and satisfies

$$\begin{aligned}&\frac{d}{dt}\mathbf{w} + \nu A\mathbf{w} + P_NB(P_N\mathbf{u},\mathbf{w}) + P_NB(\mathbf{w},\mathbf{w}) + P_NB(\mathbf{w},P_N\mathbf{u})\\ &= -\mu I_{h,N,\Omega}\mathbf{w} + \mu I_{h,N,\Omega}Q_N\mathbf{u} + P_NB(Q_N\mathbf{u},\mathbf{u}) + P_NB(P_N\mathbf{u},Q_N\mathbf{u}).\end{aligned} \tag{5.2}$$

Throughout this proof, unless otherwise noted, $\|\cdot\| = \|\cdot\|_{L^2(\Omega_0)}$. We have

$$\begin{aligned}&\frac{1}{2}\frac{d}{dt}\|\mathbf{w}\|^2 + \nu\|A^{1/2}\mathbf{w}\|^2 + (B(\mathbf{w},P_N\mathbf{u}),\mathbf{w})\\ &= -\mu(I_{h,N,\Omega}\mathbf{w},\mathbf{w}) + \mu(I_{h,N,\Omega}Q_N\mathbf{u},\mathbf{w}) + (B(Q_N\mathbf{u},\mathbf{u}) + B(P_N\mathbf{u},Q_N\mathbf{u}),\mathbf{w}),\end{aligned} \tag{5.3}$$

where we made some obvious simplifications. As in section 4 we have

$$-\mu(I_{h,N,\Omega}\mathbf{w},\mathbf{w}) = \mu(\chi_\Omega\mathbf{w} - I_{h,\Omega}(\mathbf{w}),\mathbf{w}) - \mu\int_\Omega |\mathbf{w}|^2\,d\mathbf{x} \tag{5.4}$$

and

$$|\mu(\chi_\Omega\mathbf{w} - I_{h,\Omega}(\mathbf{w}),\mathbf{w})| \le C\mu c_0 h^2\|A^{1/2}\mathbf{w}\|^2_{L^2(\Omega_0)} + \frac{\mu}{4}\|\mathbf{w}\|^2_{L^2(\Omega)}. \tag{5.5}$$

The Hölder, Ladyzhenskaya, and Young inequalities lead to

$$|(B(\mathbf{w}, P_N\mathbf{u}), \mathbf{w})| \leq \frac{C}{\nu}\|A^{1/2}\mathbf{u}\|^2\|\mathbf{w}\|^2 + \frac{\nu}{4}\|A^{1/2}\mathbf{w}\|^2. \tag{5.6}$$

Applying the spectral inequality (3.9) and using (3.2) we obtain

$$\frac{C}{\nu}\|A^{1/2}\mathbf{u}\|^2\|\mathbf{w}\|^2 \leq C\nu\lambda_1 G^2 C_\Omega e^{C_\Omega\sqrt{N}}\|\mathbf{w}\|^2_{L^2(\Omega)} \tag{5.7}$$

for sufficiently large times. Also by standard interpolation inequalities, we have

$$\begin{aligned}
&(B(Q_N\mathbf{u}, \mathbf{u}) + B(P_N\mathbf{u}, Q_N\mathbf{u}), \mathbf{w}) \\
&\quad\leq C(\|Q_N\mathbf{u}\|^{1/2}\|A^{1/2}Q_N\mathbf{u}\|^{1/2}\|\mathbf{u}\|^{1/2}\|A^{1/2}\mathbf{u}\|^{1/2} \\
&\qquad + \|P_N\mathbf{u}\|^{1/2}\|P_N A^{1/2}\mathbf{u}\|^{1/2}\|Q_N\mathbf{u}\|^{1/2}\|Q_N A^{1/2}\mathbf{u}\|^{1/2})\|A^{1/2}\mathbf{w}\| \\
&\quad\leq C\|Q_N\mathbf{u}\|^{1/2}\|A^{1/2}Q_N\mathbf{u}\|^{1/2}\|\mathbf{u}\|^{1/2}\|A^{1/2}\mathbf{u}\|^{1/2}\|A^{1/2}\mathbf{w}\| \\
&\quad\leq \frac{C}{\nu^2}\|Q_N\mathbf{u}\|\|A^{1/2}Q_N\mathbf{u}\|\|\mathbf{u}\|\|A^{1/2}\mathbf{u}\| + \frac{\nu}{4}\|A^{1/2}\mathbf{w}\|^2 .
\end{aligned}$$

Note that

$$\begin{aligned}
\frac{C}{\nu^2}\|Q_N\mathbf{u}\|\|A^{1/2}Q_N\mathbf{u}\|\|\mathbf{u}\|\|A^{1/2}\mathbf{u}\| &\leq \frac{C}{\nu^2\lambda_N^{1/2}}\|A^{1/2}\mathbf{u}\|^3\|\mathbf{u}\| \\
&\leq \frac{C}{\nu^2\lambda_N^{1/2}}(2\nu^2\lambda_1 G^2)^{3/2}(2\nu^2 G^2)^{1/2} \\
&\leq \frac{C}{\lambda_N^{1/2}}\nu^2\lambda_1^{3/2}G^4,
\end{aligned} \tag{5.8}$$

which can be made small by taking N large. Finally we have

$$\begin{aligned}
\mu|(I_{h,N,\Omega}Q_N\mathbf{u}, \mathbf{w})| &\leq \mu\|I_{h,\Omega}Q_N\mathbf{u}\|\|\chi_\Omega\mathbf{w}\| \\
&\leq \mu\|\chi_\Omega Q_N\mathbf{u}\|\|\mathbf{w}\chi_\Omega\| \leq C\mu\|\chi_\Omega Q_N\mathbf{u}\|^2 + \frac{\mu}{4}\|\mathbf{w}\|^2_{L^2(\Omega)}.
\end{aligned} \tag{5.9}$$

By our assumption on uniform Gevrey bounds for $\mathbf{u}$ we have

$$\mu\|\chi_\Omega Q_N\mathbf{u}\|^2 \leq C\mu\sum_{\sqrt{N}\lesssim|\mathbf{k}|}|\hat{\mathbf{u}}_\mathbf{k}|^2 \leq C\mu\sum_{\sqrt{N}\lesssim|\mathbf{k}|}M^2\left|\frac{L}{\mathbf{k}}\right|^2 e^{-4\pi\sigma\left|\frac{\mathbf{k}}{L}\right|},$$

and this bound holds uniformly in time for sufficiently large times. We will return to this term later after specifying a connection between μ and N.

Collecting the above estimates and dropping terms where appropriate we obtain

$$\begin{aligned}
&\frac{1}{2}\frac{d}{dt}\|\mathbf{w}\|^2 + \frac{\nu}{2}\|A^{1/2}\mathbf{w}\|^2 + \frac{\mu}{2}\int_\Omega|\mathbf{w}|^2\,d\mathbf{x} \leq C\nu\lambda_1 G^2 C_\Omega e^{C_\Omega\sqrt{N}}\|\mathbf{w}\|^2_{L^2(\Omega)} \\
&+ C\mu c_0 h^2\|A^{1/2}\mathbf{w}\|^2 + C\mu\sum_{\sqrt{N}\lesssim|\mathbf{k}|}M^2\left|\frac{L}{\mathbf{k}}\right|^2 e^{-2\pi\sigma\left|\frac{\mathbf{k}}{L}\right|} + \frac{C}{\lambda_N^{1/2}}\nu^2\lambda_1^{3/2}G^4.
\end{aligned} \tag{5.10}$$

Provided N is sufficiently large we have

$$\frac{C}{\lambda_N^{1/2}}\nu^2\lambda_1^{3/2}G^4 \leq \frac{\bar{\epsilon}}{2}. \tag{5.11}$$

Assuming this holds, let

$$\mu = 2C\nu\lambda_1 G^2 C_\Omega e^{C_\Omega\sqrt{N}} \text{ and } h_* = \sqrt{\frac{\nu}{4C\mu c_0}}$$

and take $h \leq h_*$. Then (5.10) simplifies to

$$\frac{1}{2}\frac{d}{dt}\|\mathbf{w}\|^2 + \frac{\nu}{4}\|A^{1/2}\mathbf{w}\|^2 \leq C\mu \sum_{\sqrt{N}\lesssim|\mathbf{k}|} M^2\left|\frac{L}{\mathbf{k}}\right|^2 e^{-2\pi\sigma\left|\frac{\mathbf{k}}{L}\right|} + \frac{\bar{\epsilon}}{2}. \tag{5.12}$$

Using the definition of μ in terms of N we obtain

$$\begin{aligned} C\mu \sum_{\sqrt{N}\lesssim|\mathbf{k}|} M^2\left|\frac{L}{\mathbf{k}}\right|^2 e^{-2\pi\sigma\left|\frac{\mathbf{k}}{L}\right|} &= C\nu\lambda_1 G^2 C_\Omega \sum_{\sqrt{N}\lesssim|\mathbf{k}|} M^2\left|\frac{L}{\mathbf{k}}\right|^2 e^{C_\Omega\sqrt{N}-2\pi\sigma\left|\frac{\mathbf{k}}{L}\right|} \\ &\leq \frac{C\nu\lambda_1 G^2 C_\Omega M^2}{N} \sum_{\sqrt{N}\lesssim|\mathbf{k}|} e^{C_\Omega\sqrt{N}-2\pi\sigma\left|\frac{\mathbf{k}}{L}\right|}, \end{aligned} \tag{5.13}$$

where we have hidden some global parameters. Take σ large enough so that

$$\sum_{\sqrt{N}\lesssim|\mathbf{k}|} e^{C_\Omega\sqrt{N}-2\pi\sigma\left|\frac{\mathbf{k}}{L}\right|} \leq 1.$$

This is achieved if

$$C_\Omega \lesssim \sigma.$$

In addition to (5.11), we require that

$$N \geq \frac{2C\nu\lambda_1 G^2 C_\Omega M^2}{\bar{\epsilon}}.$$

This leads to

$$\frac{1}{2}\frac{d}{dt}\|\mathbf{w}\|^2 + \frac{\nu}{4}\|A^{1/2}\mathbf{w}\|^2 \leq \bar{\epsilon}. \tag{5.14}$$

The Poincaré inequality implies

$$\frac{d}{dt}\|\mathbf{w}\|^2 + \frac{\nu}{2}\lambda_1\|\mathbf{w}\|^2 \leq 2\bar{\epsilon}. \tag{5.15}$$

By the Gronwall inequality we obtain

$$\|\mathbf{w}(t)\|^2 \leq \|\mathbf{u}_0\|^2 e^{-\nu\lambda_1 t/2} + \frac{4\bar{\epsilon}}{\nu\lambda_1}(1 - e^{-\nu\lambda_1 t/2}) \leq \|\mathbf{u}_0\|^2 e^{-\nu\lambda_1 t/2} + \frac{\epsilon}{2},$$

where we used the definition of $\bar{\epsilon}$ from the beginning of the proof. To complete the proof note that

$$\|\mathbf{u}(t)-\mathbf{v}_N(t)\|^2 \le \|\mathbf{w}(t)\|^2 + \|Q_N\mathbf{u}(t)\|^2 \le C\|\mathbf{u}_0\|^2 e^{-\nu\lambda_1 t/2} + \frac{3}{4}\epsilon,$$

provided we take N large enough so that

$$\|Q_N\mathbf{u}\|^2 \le \frac{\epsilon}{4}.$$

This plainly implies

$$\|\mathbf{u}(t)-\mathbf{v}_N(t)\| < \epsilon$$

for t sufficiently large.

The proof for $\mathcal{I}_{h,N,\Omega}$ is similar but we need to modify our treatment of (5.5) as we did at the end of the proof of Lemma 4.1. ∎

Remark 5.1. Essentially the same proof goes through for bounded domains if we use (3.10) and assume that $\mathbf{u}\cdot\phi_N$ decay sufficiently fast in N. The other modifications are standard [6].

Proof of Corollary 2.1. Let $\mathbf{v}_N$ be as in Theorem 2.1. Inspecting the proof of Theorem 2.1 we see that

$$\|\mathbf{v}_N\| \le \|\mathbf{v}_N - P_N\mathbf{u}\| + \|P_N\mathbf{u}\| < \|\mathbf{u}_0\|^2 e^{-\nu\lambda_1 t/4} + \epsilon + \|\mathbf{u}\|\,.$$

This is an upper bound for $\mathbf{v}_N$ that is time-global and independent of μ and N. For the same reason we get control of $\int_0^T\int_{\Omega_0}|\mathbf{v}_N|^2\,d\mathbf{x}\,dt$ for finite T. In contrast, the corresponding upper bounds obtained in Lemma 4.1 depended on μ and N. This implies that for any $0<\epsilon\ll 1$ we can construct a solution $\mathbf{v}_{N_\epsilon}$ for parameters N_ϵ, μ_ϵ, and h_ϵ to (2.10) with the usual energy class bounds holding independently of N_ϵ and μ_ϵ, provided we have knowledge of $\mathbf{u}$ at all points in Ω. As $\epsilon\to 0$, we have $N_\epsilon,\mu_\epsilon\to\infty$ while $h_\epsilon\to 0$. By Banach–Alaoglu, we have that there exists $\mathbf{v}$ so that $\mathbf{v}_{N_\epsilon}\to\mathbf{v}$ in the weak-star topology on $L^\infty([0,T];L^2)$ for every $T>0$ as well as the weak topology on $L^2([0,T];H^1)$.

Fix a measurable set U. Let $\Delta>0$ be a given time scale. Then for any t,

$$\int_t^{t+\Delta}\int_U(\mathbf{u}-\mathbf{v})\,d\mathbf{x}\,ds = \int_t^{t+\Delta}\int_U(\mathbf{u}-\mathbf{v}_{N_\epsilon})\,d\mathbf{x}\,ds + \int_t^{t+\Delta}\int_U(\mathbf{v}_{N_\epsilon}-\mathbf{v})\,d\mathbf{x}\,ds.$$

We have by Theorem 2.1 that

$$\begin{aligned}\int_t^{t+\Delta}\int_U(\mathbf{u}-\mathbf{v}_{N_\epsilon})\,d\mathbf{x}\,ds &\le |U|^{1/2}\left(\sup_{s\in[t,t+\Delta]}|\mathbf{u}-\mathbf{v}_{N_\epsilon}|^2(s)\right)^{1/2}\\ &\le |U|^{1/2}\left(\sup_{s\in[t,t+\Delta]}|\mathbf{u}_0|^2 e^{-\nu\lambda_1 t/4}+\frac{3}{4}\epsilon\right)^{1/2}.\end{aligned}\tag{5.16}$$

Additionally we know that

$$\left|\int_t^{t+\Delta}\int_U(\mathbf{v}_{N_\epsilon}-\mathbf{v})(\mathbf{x},t)\,d\mathbf{x}\,ds\right| \to 0$$

by $*$-weak convergence in $L^\infty L^2$. Hence we may choose ϵ so that $\epsilon < e^{-t}$ and the above quantity is smaller than e^{-t}.

By the Lebesgue differentiation theorem, for almost every t we have

$$\lim_{\Delta t\to 0}\frac{1}{\Delta t}\int_t^{t+\Delta t}\int_U (\mathbf{u}-\mathbf{v})(\mathbf{x},t)\,d\mathbf{x}\,ds = \int_U (\mathbf{u}-\mathbf{v})(\mathbf{x},t)\,d\mathbf{x},$$

where Δt is a time scale that depends on t. Let S denote the set of times for which this holds. Then $\text{meas}(S^c) = 0$ where now $\text{meas}(\cdot)$ denotes Lebesgue measure on the line. Fix $t > 0$. Then for Δt sufficiently small we have

$$\begin{aligned}
&\int_U (\mathbf{u}-\mathbf{v})(\mathbf{x},t)\,d\mathbf{x}\\
&\le \frac{1}{\Delta t}\int_t^{t+\Delta t}\int_U (\mathbf{u}-\mathbf{v})(\mathbf{x},t)\,d\mathbf{x}\,ds + e^{-t}\\
&\le \frac{1}{\Delta t}\int_t^{t+\Delta t}\int_U (\mathbf{u}-\mathbf{v}_{N_\epsilon})(\mathbf{x},t)\,d\mathbf{x}\,ds + \frac{1}{\Delta t}\int_t^{t+\Delta t}\int_U (\mathbf{v}_{N_\epsilon}-\mathbf{v})(\mathbf{x},t)\,d\mathbf{x}\,ds + e^{-t}.
\end{aligned} \tag{5.17}$$

We have already explained how the first two terms can be made exponentially small. Since this holds for all $t \in S$ we see that

$$\chi_S(t)\int_U (\mathbf{u}-\mathbf{v})(\mathbf{x},t)\,d\mathbf{x} \to 0 \tag{5.18}$$

at an exponential rate. Redefining v to equal u on S^c completes the proof.[2] ∎

Remark 5.2. The precise dynamics of $\mathbf{v}$ are unclear because we have not obtained a governing system for $\mathbf{v}$ via the limiting process. The challenge to doing so is that, as $\mu_\epsilon \to \infty$, so does $\mu_\epsilon I_{h_\epsilon,N_\epsilon,\gamma}(\mathbf{u})$. To make sense of the equations after taking limits would require $\mu_\epsilon P_{N_\epsilon} I_{h_\epsilon}(\mathbf{u}-\mathbf{v}_N{}^\epsilon)$ is bounded in some sense. Because $\mathbf{v}_N{}^\epsilon \to \mathbf{v}$, we would need $\mathbf{u} = \mathbf{v}$ for such a bound. In this case, $\mathbf{v}$ recovers the flow exactly for all times, not just as $t \to \infty$. Even granting this, the rate of convergence of $\mathbf{v}_N{}^\epsilon \to \mathbf{v}$ would need to be rapid enough to compensate for the exponential growth of μ_ϵ.

Remark 5.3. We now sketch the proof of Theorem 2.2. Granted existence, the proof follows the argument of Azouani, Olson, and Titi in [6] except we do not have a positive global term originating from the interpolant. Instead we have

$$\mu\int_\Omega |\mathbf{w}|^2\,d\mathbf{x}. \tag{5.19}$$

This and diffusion are used to hide

$$\frac{1}{2\nu}\|\mathbf{u}\|^2|\mathbf{w}|^2.$$

[2]Note that we have only used global information about u on the times in S^c, which are of measure zero. If we only want to use *local* data, then the conclusion in the statement of Corollary 2.1 can be replaced with (5.18).

Indeed, by the spectral inequality (3.11) from [78] we have

$$\frac{1}{2\nu}\|\mathbf{u}\|^2|\mathbf{w}|^2 \leq c\nu\lambda_1 G^2\left(\frac{k}{\lambda_1(\Omega_0\setminus\Omega)}\|\mathbf{w}\|^2_{L^2(\Omega)} + \frac{1}{\lambda_1(\Omega_0\setminus\Omega)}\|\mathbf{w}\|^2\right),$$

where $\lambda_1(\Omega_0\setminus\Omega)$ is the Poincaré constant for the domain $\Omega_0\setminus\Omega$ and k appears in (3.11). We require $\Omega_0\setminus\Omega$ to be thin enough that

$$\frac{c\lambda_1 G^2}{\lambda_1(\Omega_0\setminus\Omega)} \sim 1, \tag{5.20}$$

as this will allow us to hide the H^1 term in the diffusion. We then choose μ large so that the local quantity is absorbed by (5.19). Plainly this will allow us to execute the remainder of the argument from [6].

We now analyze our choice of parameters. Let h_0 be the thickness of $\Omega_0\setminus\Omega$. Then h_0 is roughly $\lambda_1(\Omega_0\setminus\Omega)^{-1/2}$. Putting this in (5.20) gives

$$h_0 \sim \frac{1}{\sqrt{\lambda_1}G}.$$

This is on the order of the length scale of the global grid in [6]. Hence, Theorem 2.2 says that it is possible to ignore roughly the outer band of observables in the volume-elements global data assimilation algorithm and still exactly recover the solution.

6. Computational results. Our computations were done on the Navier–Stokes equation in vorticity form with a fully dealiased pseudospectral code corresponding to $N\times N$ nodal values in the physical space $\Omega_0 = [0, 2\pi]^2$. The force $\mathbf{f}$, specified in Fourier space, was the same as that used in [67, 68], time independent and concentrated on the annulus with wave numbers $10 \leq |\mathbf{k}| \leq 12$. The reference solution was evolved from a zero initial value for 25,000 time units at which point the energy, enstrophy, and palinstrophy have all settled into time series for a chaotic solution (see Figure 1) with steady statistics. The viscosity was set to

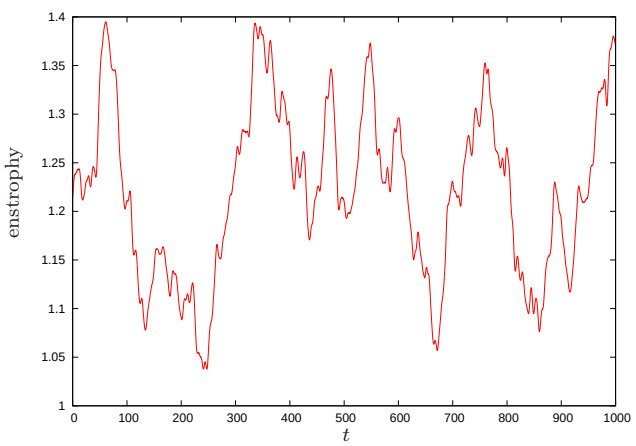

Figure 1. *Time series of enstrophy, $\|\omega_N\|^2_{L^2(\Omega_0)}$, indicating chaos.*

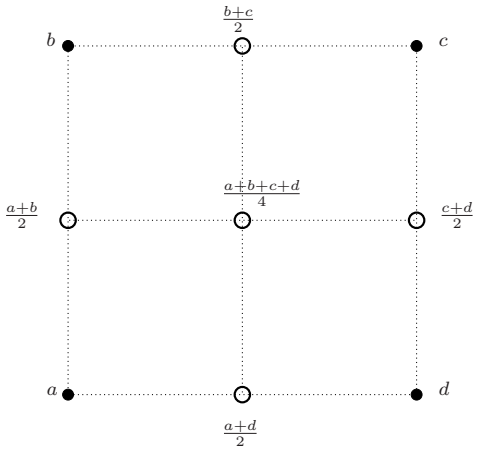

Figure 2. *First recursive step of $\mathcal{K}_p$. Values of $\tilde{\omega}_N - \omega_N$ are a, b, c, d at the corners.*

$\nu = 10^{-4}$, and a scalar multiple on the force was chosen so that the Grashof number $G = 10^6$. Both the vorticity of the reference solution $\omega_N = \nabla \times \mathbf{u}_N$ and that of the synchronizing solution $\tilde{\omega}_N = \nabla \times \mathbf{v}_N$ were solved using the third-order Adams–Bashforth method in [67, 68] in which the linear term is handled exactly through an integrating factor. The step size was $\Delta t = 0.01$ with $N = 512$, consistent with [68] at this Grashof number. We took data on square subdomains $\Omega = \Omega_j$, $j = 1, 2, 3, 4$, $\Omega_j \subset \Omega_{j-1}$, each centered in Ω_0 and with relative size

$$|\Omega_1| = 0.7656|\Omega_0|\,, \quad |\Omega_2| = 0.6602|\Omega_0|\,, \quad |\Omega_3| = 0.5265|\Omega_0|\,, \quad |\Omega_4| = 0.2500|\Omega_0|\,.$$

An interpolating operator J was computed by first applying an FFT^{-1} to the Fourier coefficients of $\tilde{\omega}_N - \omega_N$. In order to use coarse data, the resulting difference was used at only every 2^pth node in each direction, with results compared for $p = 1, 2, 3, 4$, so that $h = \pi/128, \pi/64, \pi/32$, and $\pi/16$, respectively. Before transforming back via an FFT, the field within the subdomain Ω was smoothened by the recursive averaging operator $\mathcal{K}_p$ depicted in Figure 2 and set to zero on $\Omega_0 \setminus \Omega$ so that

$$J(\tilde{\omega}_N - \omega_N) = \mathrm{FFT} \circ \chi_\Omega \circ \mathcal{K}_p \circ \mathrm{FFT}^{-1}(\tilde{\omega}_N - \omega_N)\,.$$

Note that the final transformation by the FFT serves to filter, just as P_N did in our analysis sections, though N is no longer the number of Fourier modes. After some experimentation we found taking the relaxation parameter $\mu = 50$ to be near optimal under these conditions.

We begin by testing the effect of the size of the subdomain. The relative L^2- and L^∞-norms are compared in Figure 3 with the resolution of data fixed $h = \pi/32$ ($p = 3$). To be clear, these errors are measured as

$$\frac{\|\tilde{\omega}_N - \omega_N\|_{L^2(\Omega_0)}}{\|\omega_N\|_{L^2(\Omega_0)}}, \qquad \frac{\max_{0\le j,k\le N-1} |(\tilde{\omega}_N - \omega_N)(x_j, y_k)|}{\max_{0\le m,n\le N-1} |\omega_N(x_m, y_n)|}\,,$$

respectively. In Figure 3 (as well as in Figures 4, 6, and 11) the key is arranged in the same order, top to bottom, as the error over (most of) the time interval. Machine precision is

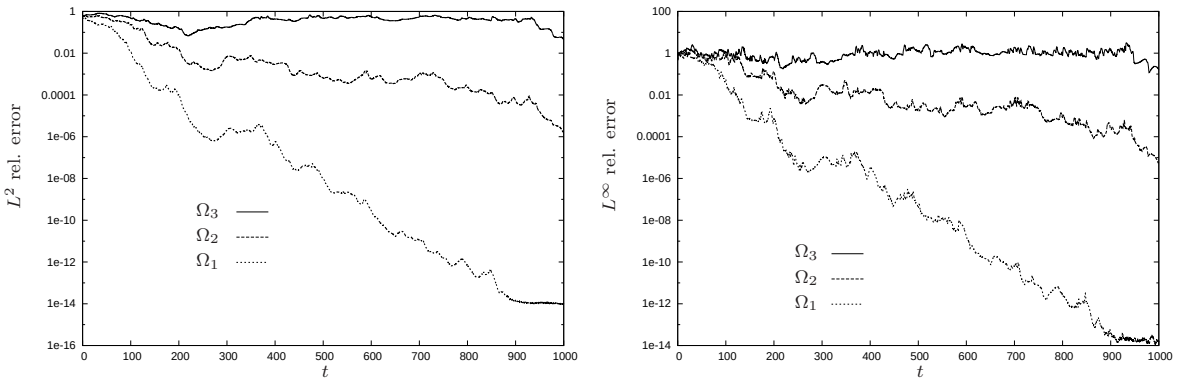

Figure 3. *Relative L^2 and L^∞ error for $\Omega = \Omega_1, \Omega_2, \Omega_3$, $p = 3$ ($h = \pi/32$).*

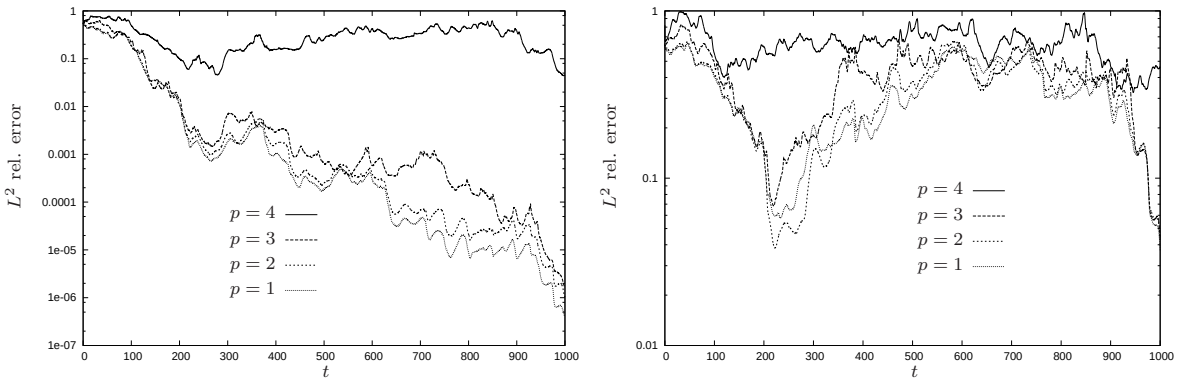

Figure 4. *Relative L^2 error for $p = 1, 2, 3, 4$. Left: $\Omega = \Omega_2$; right: $\Omega = \Omega_3$.*

reached for data collected over Ω_1 in 1000 time units. By then, in the case of Ω_2, the error is near 10^{-6}, while for Ω_3 it has barely budged from unity.

We next vary the resolution of the observed data for two subdomains, Ω_2 and Ω_3 in Figure 4. Over both subdomains there is little difference between the relative L^2 errors for $p = 1, 2, 3$. The resolution associated with $p = 4$ ($h = \pi/16$) appears to be too coarse for nudging over Ω_2 when measured in this sense. Likewise, finer resolution in the case of Ω_3 does not indicate convergence to the reference solution, at least by 1000 time units. While the relative L^2 error for $p = 4$ suggests little resemblance between $\tilde{\omega}_N$ and ω_N, particularly in the case of Ω_3, we see from the vorticity field plots in Figure 5 that the main spatial features over the full domain Ω_0 are nevertheless captured.

Since the L^2 errors over Ω_0 did not decay for data restricted to Ω_3, we cannot expect them to do so when restricting to Ω_4. We consider then relative L^2 errors that are measured also over subdomains. We found that even using data at every other node, the relative L^2 error over Ω_0 is nearly unity, after nudging all the way to $t = 10000$. In Figure 6, the plots labeled $L^2(\Omega_j)$, $j = 1, 3, 4$, are for relative errors

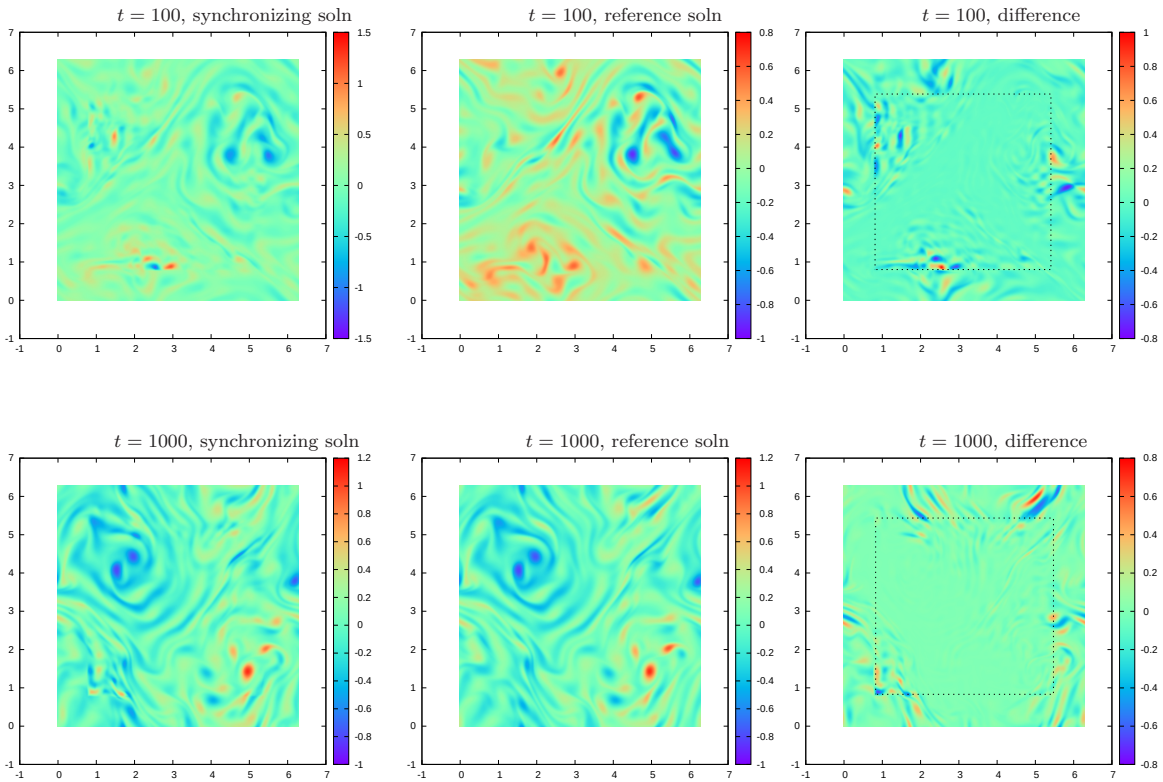

Figure 5. *Snapshots of $\tilde{\omega}_N$, ω_N and difference, for Ω_3, $p = 4$. Top: $t = 100$; bottom: $t = 1000$.*

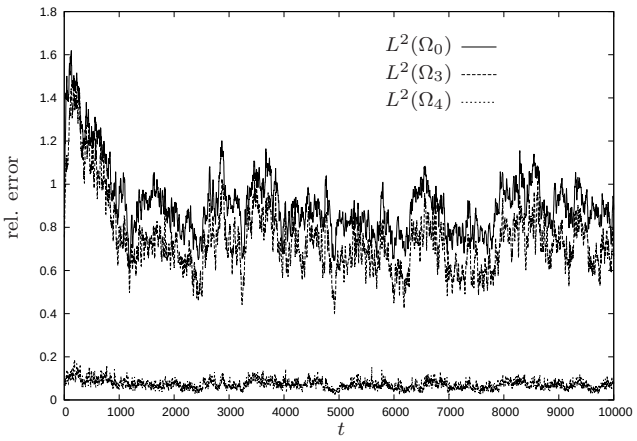

Figure 6. *Relative L^2 error over various domains, data in Ω_4, $h = \pi/128$.*

$$\frac{\|\tilde{\omega}_N - \omega_N\|_{L^2(\Omega_j)}}{\|\omega_N\|_{L^2(\Omega_j)}}.$$

The relative L^2 error over Ω_3 is nearly the same as that over Ω_0.

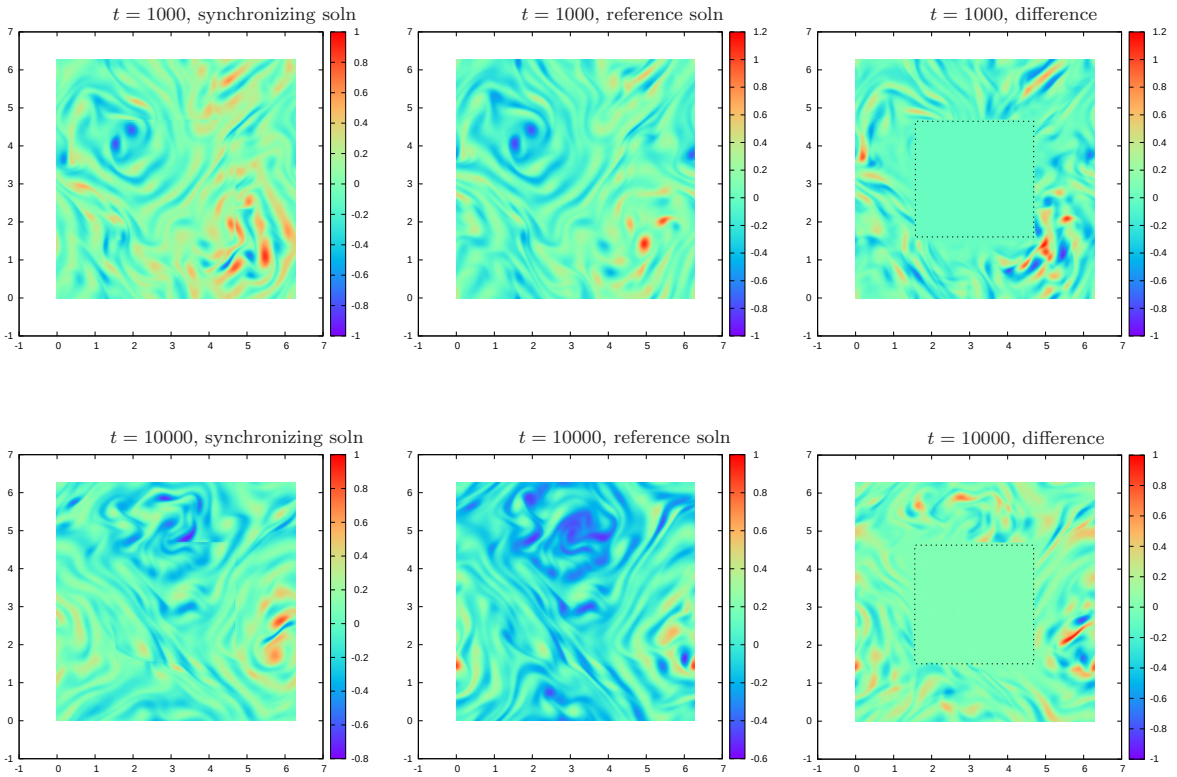

Figure 7. *Snapshots of $\tilde{\omega}_N$, ω_N and difference, for data in Ω_4, $p = 1$. Top: $t = 1000$; bottom: $t = 10000$.*

From Figure 7 we see that despite the size of these errors, again the main features of the vorticity field emerge already at $t = 1000$, but only to roughly the same extent as at $t = 10000$, consistent with the L^2 error. We also note that while the relative L^2 error over Ω_4, where the data is taken, is roughly 0.1, the plot of the difference $\tilde{\omega}_N - \omega_N$ within Ω_4 is uniformly small.

7. Mobile data. Our emphasis to this point has been on how well nudging over a fixed subdomain can recover the reference solution over the *entire* computational domain. The field plot of the difference in Figure 5 (Figure 7) shows that even with the coarsest data (smallest subdomain), the reference solution *within* the subdomain is captured well, despite the problem being global over Ω_0.

This leads us to consider moving the subdomain where the data is collected as the solution evolves. We start with $\Omega_4(t)$, a subdomain with 1/4th the area of the computational domain, specified by the location of its lower left corner (n_x, n_y) on the $N \times N$ discrete grid. The movement of the subdomain is determined by the periodic extension of the functions shown in Figure 8. The subdomain thus moves counterclockwise, covering the entire computational domain in one time unit. We fix the local interpolating operator at our most coarse setting $h = \pi/16$ ($p = 4$). The results over the initial cycle in Figure 9 show that synchronization is already well underway in just one time unit. The relative errors are plotted in Figure 11. Convergence to near machine precision is reached in one-tenth the time needed using finer data on the largest stationary subdomain, Ω_1 (compare to Figure 3).

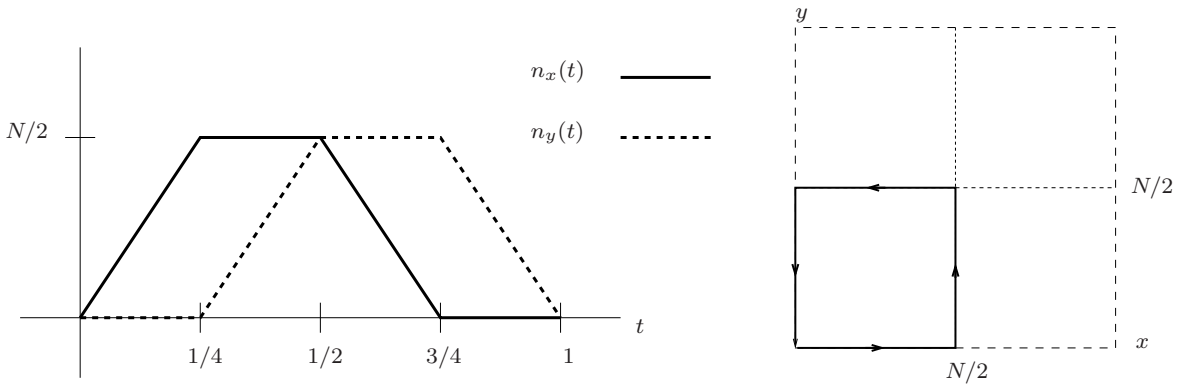

Figure 8. *Movement of lower left corner of subdomain* $\Omega_4(t)$.

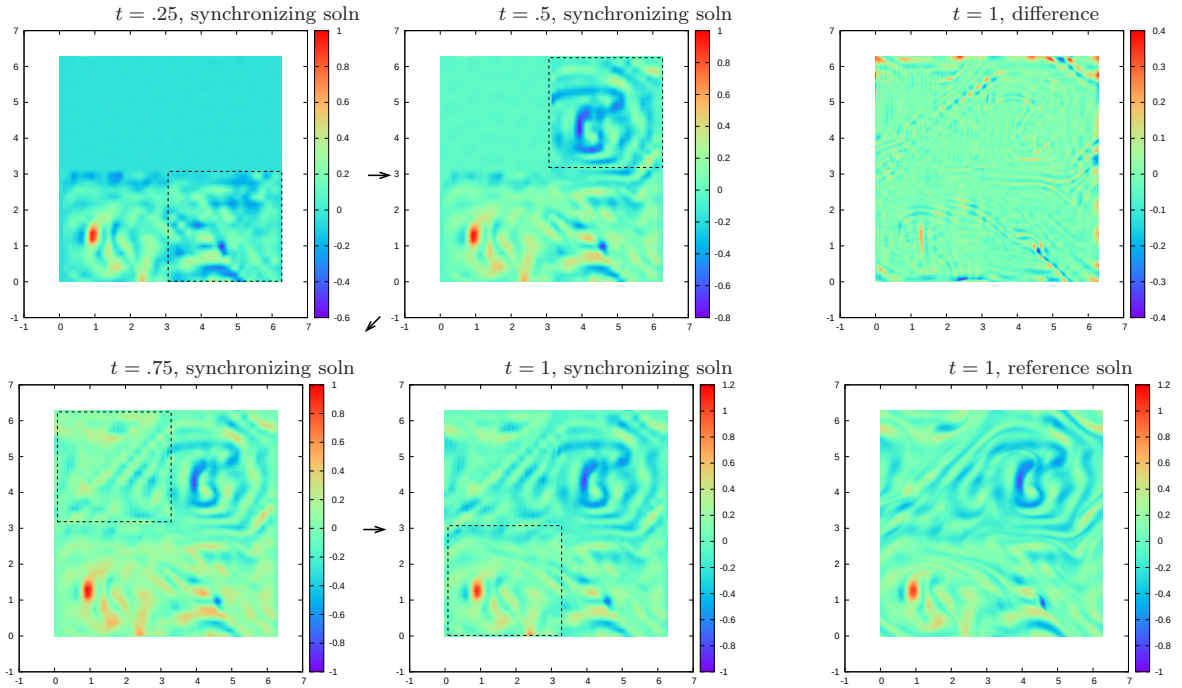

Figure 9. *Initial cycle of nudging with* $\Omega_4(t)$, $h = \pi/16$, *starting at* $t = .25$. *Reference solution and difference at* $t = 1$ *are on the right.*

A similar route can be taken by a subdomain $\Omega_5(t)$, where $|\Omega_5(t)| = 1/16|\Omega_0|$, such as that shown in Figure 10. Note that in this case the periodic extension of $n_y(t)$ is discontinuous. Though a bit slower than with $\Omega_4(t)$, synchronization is still achieved with this smallest small subdomain (see Figure 11).

8. Summary. Previous rigorous results on data assimilation in the direction of [6] rely on uniformly distributed observations of the reference solution over the full domain Ω_0. We have rigorously shown that, modulo an arbitrarily small error, the uniformly spaced observations

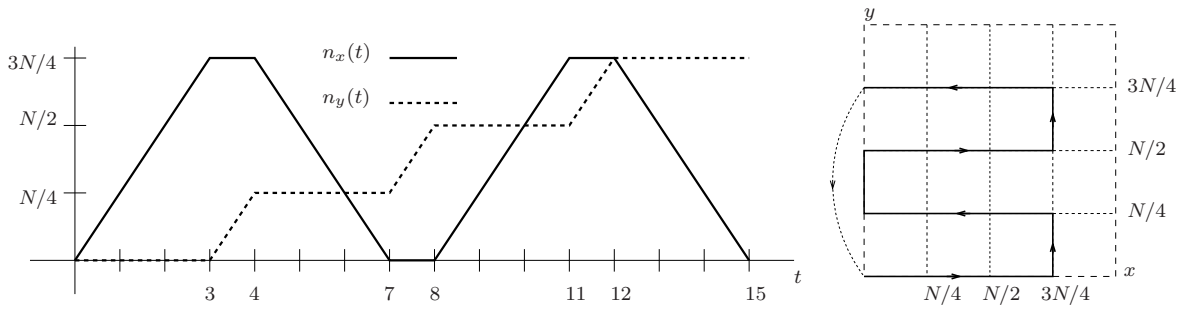

Figure 10. *Movement of lower left corner of subdomain* $\Omega_5(t)$.

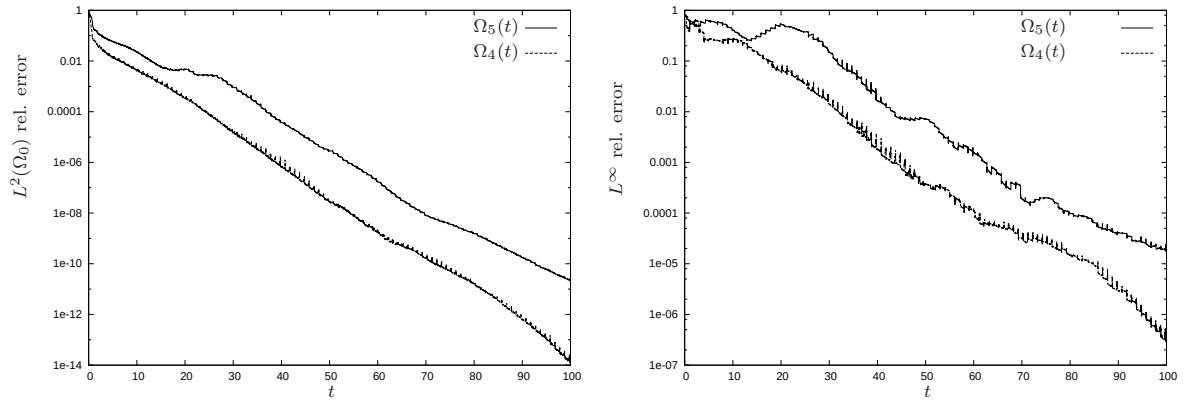

Figure 11. *Relative errors for* $\Omega_4(t)$, $\Omega_5(t)$, *both with* $h = \pi/16$.

can be confined to a subdomain provided the solution is sufficiently regular and sufficiently many local samples are used.

Analysis guarantees what should work in practice (up to numerical error). Conversely, when an algorithm works in practice, it suggests there might be some analysis to support it. Computational work has demonstrated that nudging over the entire computational domain works much better than required in the rigorous estimates [2, 67, 35, 48, 56, 57]. The conditions in Theorem 2.1 are essentially

$$\mu \gtrsim \nu G^2 e^{\sqrt{N}}, \qquad h \lesssim \sqrt{\frac{\nu}{\mu}} \sim \frac{1}{G} e^{\sqrt{N}/2}.$$

In our pseudospectral implementation, we have $h = 2\pi/N$, so strictly speaking Theorem 2.1 would require $N \sim G\exp(\sqrt{N}/2)$, which is far from obtainable.

Yet our computational results are promising. We have synchronized with a chaotic reference solution to near machine double precision in relative L^2 error using data on every eighth grid point (in each direction) on a fixed subdomain that is roughly $3/4\times$ the area of the computational domain Ω_0. The rate of exponential decay in the error slows somewhat when data is restricted to a subdomain that is roughly $2/3\times$ the area of Ω_0. The L^2 error does not appreciatively decay at all if data is taken on a subdomain of roughly $1/4\times$ the area. Still,

the main features of the vorticity field are captured if data is taken on even just a quarter of the area. Overall then, this constitutes another case of an algorithm working better than analysis suggests.

Preliminary tests of nudging on moving subdomains are even more encouraging. Sliding subdomains of $1/4\times$ and even $1/16\times$ the area of Ω_0 to cover Ω_0 achieves synchronization in one-tenth the time needed for a larger fixed domain, and does so with coarser data. This suggests analysis of mobile local data assimilation is merited, a matter we will explore in a future work.

REFERENCES

[1] D. A. F. Albanez, H. J. Nussenzveig Lopes, and E. S. Titi, *Continuous data assimilation for the three-dimensional Navier-Stokes-α model*, Asymptot. Anal., 97 (2016), pp. 139–164.

[2] M. U. Altaf, E. S. Titi, T. Gebrael, O. Knio, L. Zhao, M. F. McCabe, and I. Hoteit, *Downscaling the 2D Bénard convection equations using continuous data assimilation*, Comput. Geosci., 21 (2017), pp. 393–410.

[3] J. A. Aravequia, I. Szunyogh, E. J. Fertig, E. Kalnay, D. Kuhl, and E. J. Kostelich, *Evaluation of a strategy for the assimilation of satellite radiance observations with the local ensemble Kalman filter*, Monthly Weather Rev., 139 (2011), pp. 1932–1951.

[4] M. Asch, M. Bocquet, and M. Nodet, *Data Assimilation: Methods, Algorithms, and Applications, Fundamentals of Algorithms*, Fundam. Algorithms 11, SIAM, Philadelphia, PA, 2016.

[5] D. Auroux and J. Blum, *A nudging-based data assimilation method: The back and forth nudging (BFN) algorithm*, Nonlin. Processes Geophys., 15 (2008), pp. 305–319.

[6] A. Azouani, E. Olson, and E. Titi, *Continuous data assimilation using general interpolant observables*, J. Nonlinear Sci., 24 (2014), pp. 277–304.

[7] A. Azouani and E. S. Titi, *Feedback control of nonlinear dissipative systems by finite determining parameters—a reaction diffusion paradigm*, Evol. Equ. Control Theory, 3 (2014), pp. 579–594.

[8] H. Bae and A. Biswas, *Gevrey regularity for a class of dissipative equations with analytic nonlinearity*, Methods Appl. Anal., 22 (2015) pp. 377–408.

[9] H. Bae, A. Biswas, and E. Tadmor, *Analyticity and decay estimates of the Navier-Stokes equations in critical Besov spaces*, Arch. Ration. Mech. Anal., 205 (2012), pp. 963–991.

[10] H. Bessaih, E. Olson, and E. S. Titi, *Continuous data assimilation with stochastically noisy data*, Nonlinearity, 28 (2015), pp. 729–753.

[11] A. Biswas, C. Foias, C. F. Mondaini, and E. S. Titi, *Downscaling data assimilation algorithm with applications to statistical solutions of the Navier–Stokes equations*, Ann. Inst. H. Poincaré Anal. Non Linéaire, 36 (2019), pp. 295–326.

[12] A. Biswas, M. S. Jolly, V. R. Martinez, and E. S. Titi, *Dissipation length scale estimates for turbulent flows: A Wiener algebra approach*, J. Nonlinear Sci., 24 (2014), pp. 441–471.

[13] A. Biswas and V. R. Martinez, *Higher-order synchronization for a data assimilation algorithm for the 2D Navier–Stokes equations*, Nonlinear Anal. Real World Appl., 35 (2017), pp. 132–157.

[14] A. Biswas and D. Swanson, *Gevrey regularity of solutions to the 3-D Navier-Stokes equations with weighted l_p initial data*, Indiana Univ. Math. J., 56 (2007), pp. 1157–1188.

[15] E. Blayo, J. Verron, and J. -M. Molines, *Assimilation of TOPEX/POSEIDON altimeter data into a circulation model of the North Atlantic*, J. Geophys. Res., 99(C12), 24 691 –24 705, 1994.

[16] D. Blömker, K. Law, A. M. Stuart, and K. C. Zygalakis, *Accuracy and stability of the continuous-time 3DVAR filter for the Navier-Stokes equation*, Nonlinearity, 26 (2013), pp. 2193–2219.

[17] Z. Bradshaw, Z. Grujić, and I. Kukavica, *Local analyticity radii of solutions to the 3D Navier-Stokes equations with locally analytic forcing*, J. Differential Equations, 259 (2015), pp. 3955–3975.

[18] M. Branicki, A. J. Majda, and K. J. H. Law, *Accuracy of some approximate Gaussian filters for the Navier-Stokes equation in the presence of model error*, Multiscale Model. Simul., 16 (2018), pp. 1756–1794.

[19] M. Branicki and A. J. Majda, *An information-theoretic framework for improving imperfect dynamical predictions via multi-model ensemble forecasts*, J. Nonlinear Sci., 25 (2015), pp. 489–538.
[20] M. Branicki, B. Gershgorin, and A. J. Majda, *Filtering skill for turbulent signals for a suite of nonlinear and linear extended Kalman filters*, J. Comput. Phys., 231 (2012), pp. 1462–1498.
[21] G. Camliyurt, I. Kukavica, and V. Vicol, *Analyticity up to the boundary for the Stokes and the Navier–Stokes systems*, Trans. Amer. Math. Soc., 373 (2020), pp. 3375–3422.
[22] E. Carlson, J. Hudson, and A. Larios, *Parameter recovery for the* 2 *dimensional Navier-Stokes equations via continuous data assimilation*, SIAM J. Sci. Comput., 42 (2020), pp. A250–A270.
[23] E. Celik, E. Olson, and E. S. Titi, *Spectral filtering of interpolant observables for a discrete-in-time downscaling data assimilation algorithm*, SIAM J. Appl. Dyn. Syst., 18 (2019), pp. 1118–1142.
[24] F. W. Chaves-Silva and G. Lebeau, *Spectral inequality and optimal cost of controllability for the Stokes system*, ESAIM Control Optim. Calc. Var., 22 (2016), pp. 1137–1162.
[25] B. Cockburn, D. A. Jones, and E. S. Titi, *Determining degrees of freedom for nonlinear dissipative equations*, C. R. Acad. Sci. Paris Ser. I Math., 321 (1995), pp. 563–568.
[26] P. Constantin and C. Foias, *Navier-Stokes Equations*, Chicago Lectures in Math., University of Chicago Press, Chicago, IL, 1988.
[27] R. Daley, *Atmospheric Data Analysis*, Cambridge Atmospheric and Space Science Series, Cambridge University Press, Cambridge, UK, 1991.
[28] S. Desamsetti, H. P. Dasari, S. Langodan, E. S. Titi, O. Knio, and I. Hoteit, *Dynamical downscaling of general circulation models using continuous data assimilation*, Quart. J. Royal Meteorological Society, 145 (2019), pp. 3175–3194, https://doi.org/10.1002/qj.3612.
[29] C. Doering and E. Titi, *Exponential decay rate of the power spectrum for solutions of the Navier-Stokes equations*, Phy. Fluids, 7 (1995), pp. 1384–1390.
[30] J. Durazo, E. J. Kostelich, and A. Mahalov, *Local Ensemble Transform Kalman Filter for ionospheric data assimilation: Observation influence analysis during a geomagnetic storm event*, J. Geophysical Research Space Physics, 122 (2017), pp. 9652–9669.
[31] J. Durazo, E. J. Kostelich, A. Mahalov, and W. Tang, *Observing system experiments with an ionospheric electrodynamics model*, Phys. Scripta, 91 (2016), 044001.
[32] M. Egidi and I. Veselić, *Scale-free unique continuation estimates and Logvinenko-Sereda theorems on the torus*, Ann. Henri Poincaré, 21 (2020), pp. 3757–3790.
[33] M. Egidi and I. Veselić, *Sharp geometric condition for null-controllability of the heat equation on* R^d *and consistent estimates on the control cost*, I. Arch. Math., 111 (2018), pp. 85–99.
[34] A. Farhat, N. E. Glatt-Holtz, V. R. Martinez, S. A. McQuarrie, and J. P. Whitehead, *Data assimilation in large Prandtl Rayleigh-Bénard convection from thermal measurements*, SIAM J. Appl. Dyn. Syst., 19 (2020), pp. 510–540.
[35] A. Farhat, H. Johnston, M. S. Jolly, and E. S. Titi, *Assimilation of nearly turbulent Rayleigh-Bénard flow through vorticity or local circulation measurements: A computational study*, J. Sci. Comput., 77 (2018), pp. 1519–1533.
[36] A. Farhat, M. S. Jolly, and E. S. Titi, *Continuous data assimilation for the* 2*D Bénard convection through velocity measurements alone*, Phys. D, 303 (2015), pp. 59–66.
[37] C. Foias, O. Manley, R. Rosa, and R. Temam, *Navier–Stokes Equations and Turbulence*, Encyclopedia Math. Appl. 83. Cambridge University Press, Cambridge, UK, 2001.
[38] C. Foias, C. F. Mondaini, and E. S. Titi, *A discrete data assimilation scheme for the solutions of the two-dimensional Navier–Stokes equations and their statistics*, SIAM J. Appl. Dyn. Syst., 15 (2016), pp. 2109–2142.
[39] C. Foias and G. Prodi, *Sur le comportement global des solutions non-stationnaires des équations de Navier–Stokes en dimension* 2, Rend. Sem. Mat. Univ. Padova, 39 (1967), pp. 1–34.
[40] C. Foias and R. Temam, *Determination of the solutions of the Navier-Stokes equations by a set of nodal values*, Math. Comp., 43 (1984), pp. 117–133.
[41] C. Foias and R. Temam, *Gevrey class regularity for the solutions of the Navier-Stokes equations*, J. Funct. Anal., 87 (1989), pp. 359–369.
[42] P. K. Friz, I. Kukavica, and J. C. Robinson, *Nodal parametrisation of analytic attractors*, Discrete Contin. Dyn. Syst., 7 (2001), pp. 643–657.
[43] P. K. Friz and J. C. Robinson, *Parametrising the attractor of the two-dimensional Navier-Stokes equations with a finite number of nodal values*, Phys. D, 148 (2001), pp. 201–220.

[44] Z. Grujić and I. Kukavica, *Space analyticity for the Navier-Stokes and related equations with initial data in L^p*, J. Funct. Anal., 152 (1998), pp. 447–466.
[45] J. Harlim and A. Majda, *Filtering Complex Turbulent Systems*, Cambridge University Press, Cambridge, UK, 2012.
[46] J. Harlim and A. J. Majda, *Catastrophic filter divergence in filtering nonlinear dissipative systems*, Commun. Math. Sci., 8 (2010), pp. 27–43.
[47] J. Hoke and R. A. Anthes, *The initialization of numerical models by a dynamic initialization technique*, Monthly Weather Rev., 104 (1976), pp. 1551–1556.
[48] J. Hudson and M. S. Jolly, *Numerical efficacy study of data assimilation for the 2D magnetohydrodynamic equations*, J. Comput. Dyn., 6 (2019), pp. 131–145.
[49] M. Ignatova and I. Kukavica, *Strong unique continuation for the Navier-Stokes equation with nonanalytic forcing*, J. Dynam. Differential Equations, 25 (2013), pp. 1–15.
[50] D. A. Jones and E. S. Titi, *Upper bounds on the number of determining modes, nodes, and volume elements for the Navier-Stokes equations*, Indiana Univ. Math. J., 42 (1993), pp. 875–887.
[51] E. Kalnay, *Atmospheric Modeling, Data Assimilation and Predictability*, Cambridge University Press, Cambridge, UK, 2003.
[52] D. T. B. Kelly, K. J. H. Law, and A. M. Stuart, *Well-posedness and accuracy of the ensemble Kalman filter in discrete and continuous time*, Nonlinearity, (2014), pp. 2579–2603.
[53] O. Kovrijkine, *Some results related to the Logvinenko-Sereda theorem*, Proc. Amer. Math. Soc., 129 (2001), pp. 3037–3047.
[54] E. J. Kostelich, Y. Kuang, J. McDaniel, N. Z. Moore, N. L. Martirosyan, and M. C. Preul, *Accurate state estimation from uncertain data and models: An application of data assimilation to mathematical models of human brain tumors*, Biology Direct (2011).
[55] I. Kukavica, *On the dissipative scale for the Navier-Stokes equation*, Indiana Univ. Math. J., 48 (1999), pp. 1057–1081.
[56] A. Larios, L. G. Rebholz, and C. Zerfas, *Global in time stability and accuracy of IMEX-FEM data assimilation schemes for Navier-Stokes equations*, Comput. Methods Appl. Mech. Engrg., 345 (2019), pp. 1077–1093.
[57] A. Larios and C. Victor, *Continuous data assimilation with a moving cluster of data points for a reaction diffusion equation: A computational study*, Commun. Comput. Phys., 29 (2021), pp. 1273–1298.
[58] K. Law, A. M. Stuart, and K. C. Zygalakis, *Data Assimilation: A Mathematical Introduction*, Springer, New York, 2015.
[59] J. McDaniel, E. J. Kostelich, Y. Kuang, J. Nagy, M. C. Preul, N. Z. Moore, and N. L. Matirosyan, *Data assimilation in brain tumor models*, in Mathematical Methods and Models in Biomedicine, Springer, Berlin, 2013, pp. 233–262.
[60] J. Le Rousseau and G. Lebeau, *On Carleman estimates for elliptic and parabolic operators. Applications to unique continuation and control of parabolic equations*, ESAIM Control Optim. Calc. Var., 18 (2012), pp. 712–747.
[61] G. Lebeau and L. Robbiano, *Contrôle exact de l'équation de la chaleur*, Comm. Partial Differential Equations, 20 (1995), pp. 335–356.
[62] G. Lebeau and E. Zuazua, *Null-controllability of a system of linear thermoelasticity*, Arch. Ration. Mech. Anal., 141 (1998), pp. 297–329.
[63] D. Luenberger, *An introduction to observers*, IEEE Trans. Automat. Control, 16 (1971), pp. 596–602.
[64] P. A. Markowich, E. S. Titi, and S. Trabelsi, *Continuous data assimilation for the three-dimensional Brinkman-Forchheimer-extended Darcy model*, Nonlinearity, 29 (2016), pp. 1292–1328.
[65] H. Nijmeijer, *A dynamic control view of synchronization*, Phys. D, 154 (2001), pp. 219–228.
[66] M. Oliver and E. Titi, *On the domain of analyticity for solutions of second order analytic nonlinear differential equations*, J. Differential Equations, 174 (2001), pp. 55–74.
[67] E. Olson and E. S. Titi, *Determining modes for continuous data assimilation in 2D turbulence*, J. Statist. Phys., 113 (2003), pp. 799–840.
[68] E. Olson and E. S. Titi, *Determining modes and Grashof number in 2D turbulence: A numerical study*, Theoret. Comput. Fluid Dyn., 22 (2008), pp. 327–339.
[69] L. M. Pecora and T. L. Carroll, *Synchronization of Chaotic Systems*, Chaos, 25 (2015), 097611.

[70] S. Reich and C. Cotter, *Probabilistic Forecasting and Bayesian Data Assimilation*, Cambridge University Press, Cambridge, UK, 2015.
[71] D. R. Stauffer and N. L. Seaman, *Use of four dimensional data assimilation in a limited area mesoscale model. Part* 1: *Experiments with synoptic-scale data*, Monthly Weather Rev., 118 (1990), pp. 1250–1277.
[72] C. A. Stewart, V. Welch, B. Plale, G. Fox, M. Pierce, and T. Sterling, *Indiana University Pervasive Technology Institute*, 2017, https://doi.org/10.5967/K8G44NGB.
[73] R. Temam, *Navier-Stokes Equations. Theory and Numerical Analysis*, AMS Chelsea, Providence, RI, 2001.
[74] F. E. Thau, *Observing the state of non-linear dynamic systems*, Internat. J. Control, 17 (1973), pp. 471–479.
[75] X. T. Tong, A. J. Majda, and D. Kelly, *Nonlinear stability of the ensemble Kalman filter with adaptive covariance inflation*, Commun. Math. Sci., 14 (2016), pp. 1283–1313.
[76] X. T. Tong, A. J. Majda, and D. Kelly, *Nonlinear stability and ergodicity of ensemble based Kalman filters*, Nonlinearity, 29 (2016), pp. 657–691.
[77] J. Verron, *Altimeter data assimilation into an ocean circulation model: Sensitivity to orbital parameters*, J. Geophys. Res., 95 (1990), pp. 443–459.
[78] X. Yu and Y. Li, *The Stabilization of the FitzHugh-Nagumo Systems with One Feedback Controller*, Proceedings of the 27th Chinese Control Conference, Kunming, 2008, pp. 417–419, https://doi.org/10.1109/CHICC.2008.4605695.